

## Discovery and Metabolic Stabilization of Potent and Selective 2-Amino-*N*-(adamant-2-yl) Acetamide 11 $\beta$ -Hydroxysteroid Dehydrogenase Type 1 Inhibitors

Jeffrey J. Rohde,<sup>\*,†</sup> Marina A. Pliushchev,<sup>†</sup> Bryan K. Sorensen, Dariusz Wodka,<sup>‡</sup> Qi Shuai, Jiahong Wang, Steven Fung, Katina M. Monzon, William J. Chiou, Liping Pan,<sup>§</sup> Xiaoqing Deng,<sup>§</sup> Linda E. Chovan,<sup>‡</sup> Atul Ramaiya,<sup>§</sup> Mark Mullally,<sup>‡</sup> Rodger F. Henry,<sup>||</sup> DeAnne F. Stolarik,<sup>⊥</sup> Hovis M. Imade,<sup>⊥</sup> Kennan C. Marsh,<sup>⊥</sup> David W. A. Beno,<sup>⊥</sup> Thomas A. Fey, Brian A. Droz, Michael E. Brune, Heidi S. Camp, Hing L. Sham, Ernst Uli Frevert,<sup>#</sup> Peer B. Jacobson, and J. T. Link<sup>†</sup>

Metabolic Disease Research, Abbott Laboratories, 200 Abbott Park Road, Department R4CB, Building AP52, Abbott Park, Illinois 60064-3500

Received August 2, 2006

Starting from a rapidly metabolized adamantane 11 $\beta$ -hydroxysteroid dehydrogenase type 1 (11 $\beta$ -HSD1) inhibitor **22a**, a series of *E*-5-hydroxy-2-adamantamine inhibitors, exemplified by **22d** and ( $\pm$ )-**22f**, was discovered. Many of these compounds are potent inhibitors of 11 $\beta$ -HSD1 and are selective over 11 $\beta$ -HSD2 for multiple species (human, mouse, and rat), unlike other reported species-selective series. These compounds have good cellular potency and improved microsomal stability. Pharmacokinetic profiling in rodents indicated moderate to large volumes of distribution, short half-lives, and a pharmacokinetic species difference with the greatest exposure measured in rat with **22d**. One hour postdose liver, adipose, and brain tissue 11 $\beta$ -HSD1 inhibition was confirmed with ( $\pm$ )-**22f** in a murine *ex vivo* assay. Although 5,7-disubstituted-2-adamantamines provided greater stability, a single, *E*-5-position, polar functional group afforded inhibitors with the best combination of stability, potency, and selectivity. These results indicate that adamantane metabolic stabilization sufficient to obtain short-acting, potent, and selective 11 $\beta$ -HSD1 inhibitors has been discovered.

### Introduction

The predominant therapeutic strategy for preventing, or managing, type 2 diabetes and cardiovascular disease is the individual treatment of a set of risk factors including elevated fasting plasma glucose, elevated triglycerides, elevated blood pressure, reduced high-density lipoprotein (HDL<sup>c</sup>) cholesterol, and central obesity.<sup>1</sup> When central obesity and two of the other four risk factors are present in a single patient, the individual, by definition, has the metabolic syndrome (MetS).<sup>2</sup> Patients with Cushing's disease have elevated levels of circulating glucocorticoids (GCs) and exhibit similar, but more profound, symptoms compared to those with MetS.<sup>3</sup> Cushing's disease can be reversed by normalization of GC levels.<sup>4</sup> Based upon this observation, it is tempting to speculate that MetS is driven by GCs and could be treated by suppression of their action. However, circulating levels of GCs are not elevated in patients with MetS.<sup>5</sup> It has also been hypothesized that intracellular levels of GC may be elevated in patients with MetS and may be responsible for the shared features with Cushing's patients. Although this has not been demonstrated, suppression of GC action may, nevertheless, result in a desirable clinical response.<sup>6</sup>

Two isoforms of the 11 $\beta$ -hydroxysteroid dehydrogenase enzymes, type 1 (11 $\beta$ -HSD1) and type 2 (11 $\beta$ -HSD2), regulate intracellular levels of GCs.<sup>7</sup> 11 $\beta$ -HSD1 is a low affinity reductase that converts glucocorticoid receptor (GR) inactive cortisone into GR active cortisol (11-dehydrocorticosterone and corticosterone, respectively, in rodents).<sup>8</sup> 11 $\beta$ -HSD1 is expressed in liver, adipose, brain, and many other tissues and increases the intracellular levels of active GCs. Thus, inhibiting 11 $\beta$ -HSD1 is an approach for suppressing GC action. 11 $\beta$ -HSD2 is a high affinity oxidase that inactivates GCs by catalyzing the reverse reaction in mineralocorticoid (MC) sensitive tissues, such as the kidney and colon.<sup>9</sup> The mineralocorticoid receptor (MR) has equal functional affinity for cortisol and its native ligand, aldosterone, which regulates blood pressure and sodium balance in the kidney.<sup>10</sup> Patients with apparent mineralocorticoid excess (AME), caused by loss of 11 $\beta$ -HSD2 function, have hypertension due to kidney MR activation by cortisol.<sup>11</sup> Consequently, inhibitors for 11 $\beta$ -HSD1 must be selective over 11 $\beta$ -HSD2.

Murine genetic experiments indicate that reduced 11 $\beta$ -HSD1 expression can produce metabolically significant beneficial effects on MetS risk factors and that tissue specificity is of importance. Genetic ablation of 11 $\beta$ -HSD1 in mice reduces the metabolic consequences of obesity, improves hepatic insulin sensitivity, lowers plasma triglycerides, increases HDL cholesterol, and protects against hyperglycemia.<sup>12</sup> High fat feeding of the 11 $\beta$ -HSD1<sup>-/-</sup> mice is associated with "favorable" altered fat distribution, improved adipose insulin sensitivity, and resistance to diet-induced metabolic syndrome.<sup>13</sup> Overexpression of 11 $\beta$ -HSD1 in adipose tissue of mice to levels comparable to that measured in the adipose tissue of obese humans induced central obesity, insulin resistance, hypertension, and dyslipidemia.<sup>14</sup> However, liver specific overexpression of 11 $\beta$ -HSD1 resulted in no change in fat mass and mild insulin resistance, but did result in reduced hepatic lipid clearance.<sup>15</sup> Overexpression of 11 $\beta$ -HSD2 in adipose tissue, analogous to adipose selective 11 $\beta$ -HSD1 inhibition, protected the mice against diet-

\* To whom correspondence should be addressed. Phone: (847) 935-5092. Fax: (847) 938-3403. E-mail: jeffrey.j.rohde@abbott.com.

<sup>†</sup> Equal contributors.

<sup>‡</sup> Medicinal Chemistry Technologies.

<sup>§</sup> Drug Metabolism.

<sup>||</sup> Structural Chemistry.

<sup>⊥</sup> Exploratory Science.

<sup>#</sup> Novartis Pharmaceuticals, East Hanover, NJ; uli.frevert@novartis.com.

<sup>a</sup> Abbreviations: 11 $\beta$ -HSD1, 11 $\beta$ -hydroxysteroid dehydrogenase type 1; 11 $\beta$ -HSD2, 11 $\beta$ -hydroxysteroid dehydrogenase type 2; HDL, high density lipoprotein; MetS, metabolic syndrome; GCs, glucocorticoids; GR, glucocorticoid receptor; MC, mineralocorticoid; MR, mineralocorticoid receptor; AME, apparent mineralocorticoid excess; HPA, hypothalamic-pituitary-adrenal; TosMIC, *p*-toluenesulfonylmethyl isocyanide; DAST, (diethylamino)sulfur trifluoride; SPA, scintillation proximity assay; FPIA, fluorescence polarization immuno-assay; HSD1, 11 $\beta$ -HSD1; HSD2, 11 $\beta$ -HSD2; h-, human; m-, mouse; r-, rat; HLM, human liver microsomes; MLM, mouse liver microsomes; RLM, rat liver microsomes.

induced obesity.<sup>16</sup> Furthermore, there is an adaptive down-regulation of adipose 11 $\beta$ -HSD1 expression in both MetS prone and resistant strains of mice on a high-fat diet.<sup>17</sup> Thus, genetic experiments in mice support selective inhibition of 11 $\beta$ -HSD1 as a therapeutic target for the treatment of MetS and emphasize the likely requirement of adipose tissue inhibition for efficacy.

In humans the evidence that 11 $\beta$ -HSD1 inhibition will be a successful therapy for the treatment of MetS has been more difficult to obtain and is weaker than for rodents. In human adipocytes, 11 $\beta$ -HSD1 mRNA levels and enzyme activity were either increased<sup>18</sup> or unchanged<sup>19</sup> by obesity, while hepatic 11 $\beta$ -HSD1 activity was reduced.<sup>20</sup> In isotope dilution studies with deuterium-labeled cortisol, cortisol production rates were increased with increasing percentage body fat, but due to increased cortisol clearance rates, plasma-free cortisol levels were independent of body composition. However, both cortisol production rates and plasma free cortisol levels did increase with increasing age.<sup>21</sup> More recently, additional isotope tracer studies have been performed to further investigate changes in cortisol metabolism caused by obesity and diabetes.<sup>22</sup> In healthy volunteers, cortisol production by the splanchnic bed, including both the liver and the visceral adipose tissue, is greater than, or equal to, extrasplanchnic cortisol production (primarily the adrenal glands) throughout the day.<sup>22b</sup> Adipose tissue contributes approximately two-thirds to this cortisol production.<sup>22c</sup> However, net cortisol release from the splanchnic bed is minimal due to concurrent splanchnic cortisol uptake. Surprisingly, the rates of splanchnic cortisol production are not altered in obese or diabetic patients.<sup>22d</sup> However, obesity, with increased visceral adiposity, does increase splanchnic cortisol uptake. The overall relationship between 11 $\beta$ -HSD1 activity, obesity, and diabetes in humans remains largely unknown and speculation is primarily based upon analogy with rodent models. Current human data suggests targeting inhibition of 11 $\beta$ -HSD1 activity in adipose tissue will be beneficial.

The effect of 11 $\beta$ -HSD1 inhibition on the hypothalamic-pituitary-adrenal (HPA) axis in humans is unknown.<sup>1c</sup> Genetic studies in rodents suggest mild activation of the HPA axis and that tissue selective inhibition may reduce or eliminate this effect. While the primary function of the HPA axis is to regulate the circadian and stress-induced synthesis of cortisol, it is also responsible for regulating MC precursors and adrenal androgens.<sup>23</sup> As a consequence, activation of the HPA axis may produce adverse effects due to MC and/or androgen<sup>24</sup> excess. In 11 $\beta$ -HSD1 null mice, adrenal hyperplasia was observed,<sup>12,25</sup> but this condition was eliminated by the addition of liver specific 11 $\beta$ -HSD1 expression.<sup>26</sup> And, when 11 $\beta$ -HSD2 was overexpressed in adipose tissue of mice, analogous to an adipose selective 11 $\beta$ -HSD1 inhibitor, there was no change in serum corticosterone levels or adrenal weights.<sup>16</sup> The effect of an 11 $\beta$ -HSD1 inhibitor on the human HPA axis can only be determined clinically, and based on the previous studies, adipose tissue should be the primary target of 11 $\beta$ -HSD1 inhibition.

Unselective and selective inhibitors of 11 $\beta$ -HSD1 have been studied in rodent models of diabetes and humans. Carbenoxolone **1** (Figure 1), a potent, nonselective 11 $\beta$ -HSD1 and 11 $\beta$ -HSD2 steroid inhibitor, displayed modest efficacy when evaluated in models of diabetes and obesity.<sup>27</sup> Carbenoxolone has been studied in obese insulin resistant Zucker rats, a strain that displays increased adipose activity and decreased liver activity of 11 $\beta$ -HSD1, similar to obese human patients.<sup>27a</sup> Only liver inhibition of 11 $\beta$ -HSD1 activity was measurable in *ex vivo* tissue 11 $\beta$ -HSD1 activity studies (not adipose or muscle). Increased HDL cholesterol and plasma insulin response to glucose were

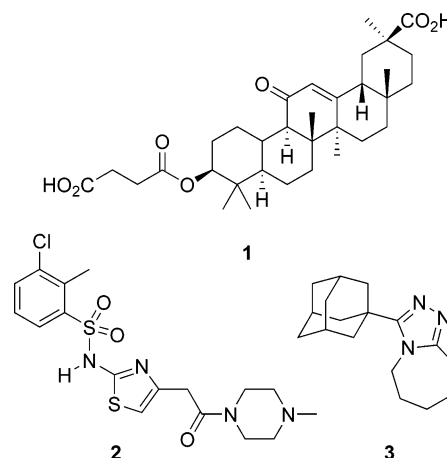
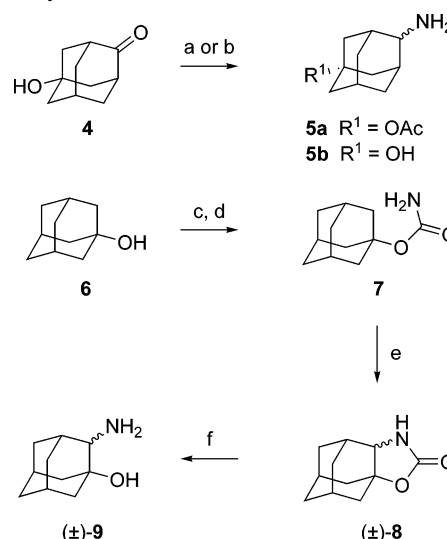


**Figure 1.** The 11 $\beta$ -HSD1 inhibitors carbenoxolone (**1**), BVT.2733 (**2**), and compound 554 (**3**).

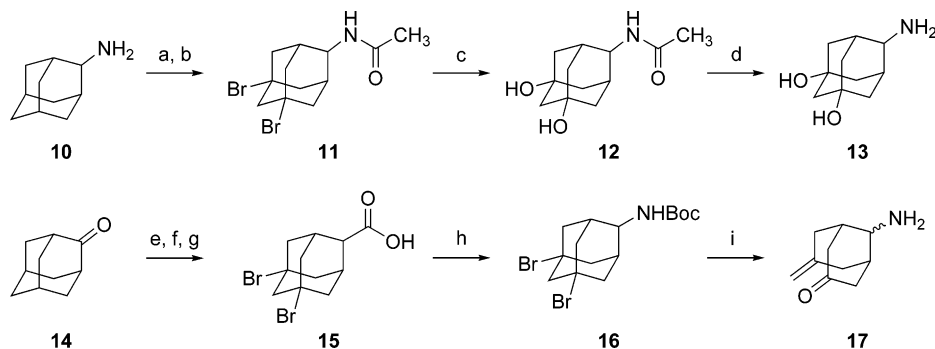
**Scheme 1.** Syntheses of Disubstituted Adamantane Amines<sup>a</sup>



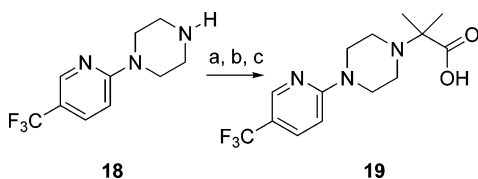
<sup>a</sup> Reagents and conditions: (a) acetic anhydride, DMAP, CH<sub>2</sub>Cl<sub>2</sub>, 50 °C, 16 h, 96%; NH<sub>3</sub>, 4 Å MS, NaBH<sub>4</sub>, MeOH, 23 °C, 16 h, 58%; (b) NH<sub>3</sub>, 4 Å MS, NaBH<sub>4</sub>, MeOH, 0 °C → 23 °C, 18 h, 98%; (c) Cl<sub>3</sub>CCONCO, CH<sub>2</sub>Cl<sub>2</sub>, 0 °C → 23 °C, 2 h; (d) K<sub>2</sub>CO<sub>3</sub>, MeOH, 50 °C, 16 h, 87%; (e) PhI(OAc)<sub>2</sub>, MgO, (Rh(OAc)<sub>2</sub>)<sub>2</sub>, CH<sub>2</sub>Cl<sub>2</sub>, 50 °C, 4 h, 69%; (f) 5 N KOH, dioxane, 70 °C, 16 h, 87%.

observed. No effect on weight gain, food intake, or plasma glucose on oral glucose tolerance testing was measured. In a one week study in healthy human volunteers with oral administration, carbenoxolone improved insulin sensitivity and reduced glucose production.<sup>27b</sup> However, long term oral administration of carbenoxolone with co-administration of amelioration (to prevent renal mineralocorticoid excess due to 11 $\beta$ -HSD2 activity) gave no change in glycemic control, serum lipid profile, or plasma cortisol with this unselective 11 $\beta$ -HSD1 inhibitor.<sup>27c</sup>

The first reported potent and selective murine 11 $\beta$ -HSD1 inhibitor, **2**, showed efficacy *in vivo* in several mouse models.<sup>28</sup> In KKA<sup>y</sup> mice with oral dosing, this compound dose-dependently lowered blood glucose levels. In a one week, osmotic minipump study with sustained inhibition, **2** not only lowered blood glucose levels but also serum insulin concentrations and mRNA levels of key gluconeogenic liver enzymes.<sup>28a,b</sup> Additional studies in *db/db* mice demonstrated reduced glucose and insulin levels upon oral dosing of compound. And, similar dosing of *ob/ob* mice lead to reduced food intake, body weight, glucose, and insulin, as well as improved glycemic control in response to an oral glucose tolerance test.<sup>28c</sup> Only hepatic 11 $\beta$ -

Scheme 2. Syntheses of Trisubstituted Adamantane Amines<sup>a</sup>

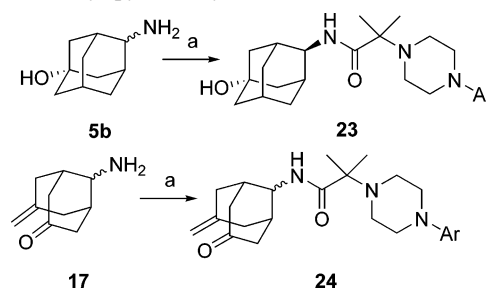
<sup>a</sup> Reagents and conditions: (a) acetic anhydride, pyridine, 23 °C, 16 h; (b) Br<sub>2</sub>, AlBr<sub>3</sub>, 90 °C, 7 days, 21%; (c) AgSO<sub>4</sub>, conc. H<sub>2</sub>SO<sub>4</sub>, H<sub>2</sub>O, 80 °C, 2 h, 70%; (d) 6 N HCl, H<sub>2</sub>O, 80 °C, 16 h, 99%; (e) TosMIC, *t*-BuOK, DME, EtOH, 5 °C → 40 °C, 1 h, 98%; (f) HBr, AcOH, 120 °C, 16 h, 92%; (g) AlBr<sub>3</sub>, Br<sub>2</sub>, 0 °C → 70 °C, 20 h, 74%; (h) DPPA, TEA, toluene, *t*-BuOH, reflux, 24 h, 44%; (i) NaOH, dioxane, microwave, 180 °C, 15 min.

Scheme 3. Sidechain Synthesis<sup>a</sup>

<sup>a</sup> Reagents and conditions: (a) methyl 2-bromopropionate, DIPEA, MeOH, 70 °C, 16 h, 99%; (b) LDA, MeI, THF, -65 °C → 23 °C, 3 h, 82%; (c) 5 N KOH, dioxane, 60 °C, 4 h, 90%.

HSD1 tissue activity was reported for **2**, making it difficult to determine the importance of adipose tissue activity to the observed efficacy. Recently, a dual mouse and human potent and selective HSD1 inhibitor, compound **3**, was reported.<sup>29</sup> This triazole lowered body weight, insulin, fasting glucose, triglycerides, and cholesterol in diet-induced obese C57BL/6J mice.<sup>29b</sup> Oral dosing of **3** in high-fat fed and streptozotocin-treated ICR mice also lowered fasting glucose, insulin, glucagon, triglycerides, and free fatty acids, as well as improved glucose tolerance. Inhibition of 11 $\beta$ -HSD1 activity was reported in liver, epididymal white adipose, and brain tissues.<sup>29b</sup> Thus, significant and desirable therapeutic modifications have been demonstrated on important MetS risk factors in murine models of obesity and type 2 diabetes by selective inhibition of 11 $\beta$ -HSD1, particularly upon sustained administration.

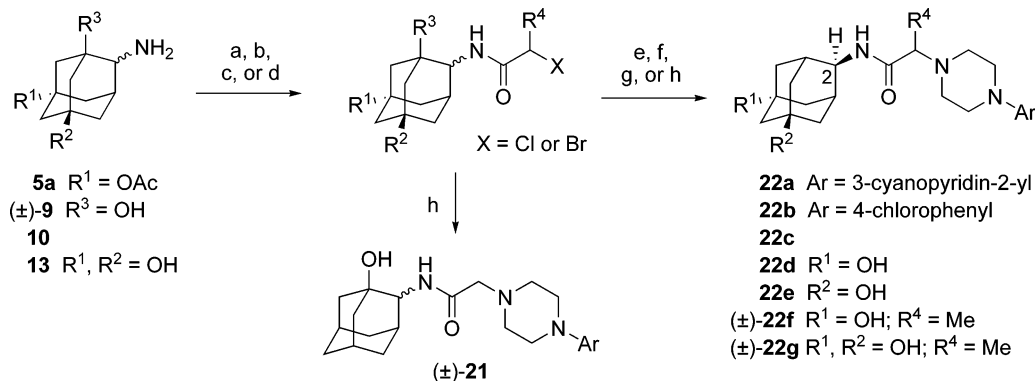
11 $\beta$ -HSD1 inhibition is also being investigated for other indications including cognition,<sup>27c,30</sup> glaucoma,<sup>31</sup> atheroscler-

Scheme 5. Adamantane Sidechain Attachments Wherein Ar = 5-Trifluoromethyl-pyridin-2-yl<sup>a</sup>

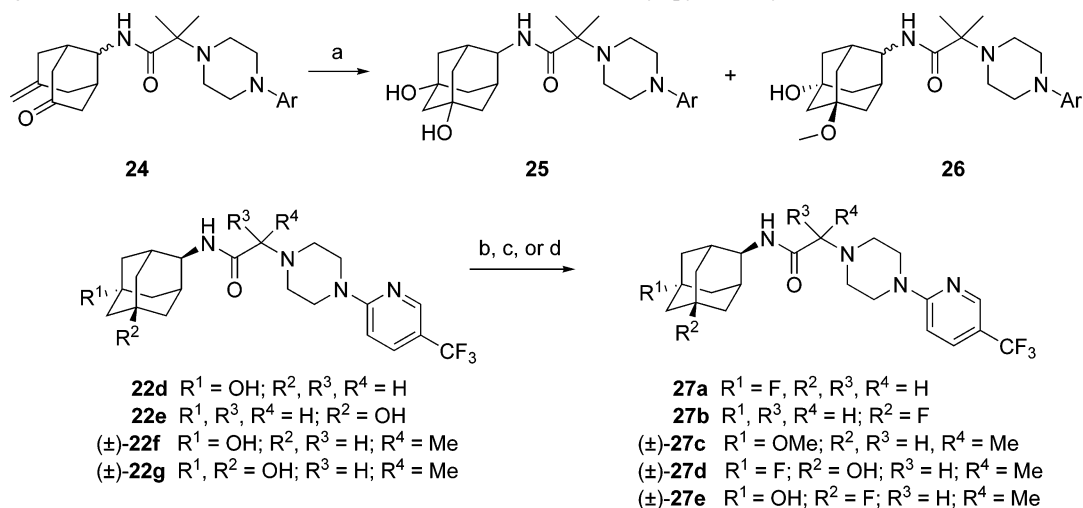
<sup>a</sup> Reagents and conditions: (a) **19**, EDCl, HOBt, DIPEA, CH<sub>2</sub>Cl<sub>2</sub>, 23 °C; 16 h, **23** (69%), **24** (65%).

osis,<sup>29b,32</sup> osteoporosis,<sup>33</sup> wound healing,<sup>34</sup> and other disorders that are anticipated to improve with reduced GC action.<sup>35</sup> Further study of 11 $\beta$ -HSD1 inhibition for MetS or other indications can greatly be advanced by the preparation of isoform selective 11 $\beta$ -HSD1 inhibitors. Specifically for the treatment of the MetS, the rodent validation points to sustained inhibition of 11 $\beta$ -HSD1 within adipose tissue as the primary target for efficacy and safety. Accordingly, a program designed to test this hypothesis was initiated. Herein we report the discovery of potent and isoform selective, human 11 $\beta$ -HSD1 adamantane inhibitors with potent cellular activity and tissue penetration.

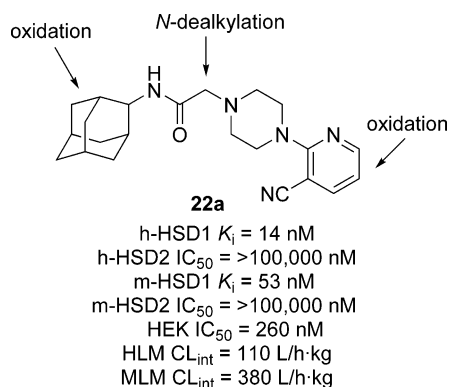
**Synthesis of 2-Amino-*N*-(adamant-2-yl) Acetamides.** 2,5- and 1,2-Disubstituted adamantanes were prepared by two

Scheme 4. Adamantane Sidechain Attachments Wherein R<sup>1</sup>, R<sup>2</sup>, R<sup>3</sup>, and R<sup>4</sup> = H and Ar = 5-trifluoromethyl-pyridin-2-yl Unless Specified<sup>a</sup>

<sup>a</sup> Reagents and conditions: (a) bromoacetyl chloride, 2 N NaOH, CH<sub>2</sub>Cl<sub>2</sub>, 23 °C, 1 h, 68%; (b) chloroacetyl chloride, DIPEA, CH<sub>2</sub>Cl<sub>2</sub>, 0 °C → 23 °C, 2 h, 92%; (c) 2-bromopropionyl chloride, DIPEA, CH<sub>2</sub>Cl<sub>2</sub>, 0 °C → 23 °C, 2 h, 84%; (d) 2-bromopropionyl chloride, NaHCO<sub>3</sub>, H<sub>2</sub>O, 0 °C → 23 °C, 16 h, 36%; (e) 1-(3-cyanopyridin-2-yl)piperazine, DIPEA, toluene, 60 °C, 18 h, 82%; (f) 1-(4-chlorophenyl)piperazine, DIPEA, MeOH, 70 °C, 16 h, 65%; (g) 1-(5-trifluoromethyl-pyridin-2-yl)piperazine, DIPEA, MeOH, 70 °C, 16 h, 71%; (h) 1-(5-trifluoromethyl-pyridin-2-yl)piperazine, DIPEA, MeOH, 70 °C, 16 h; K<sub>2</sub>CO<sub>3</sub>, H<sub>2</sub>O, 70 °C, 16 h, 46%.

**Scheme 6.** 11 $\beta$ -HSD1 Inhibitor Modifications Wherein Ar = 5-Trifluoromethyl-pyridin-2-yl<sup>a</sup>

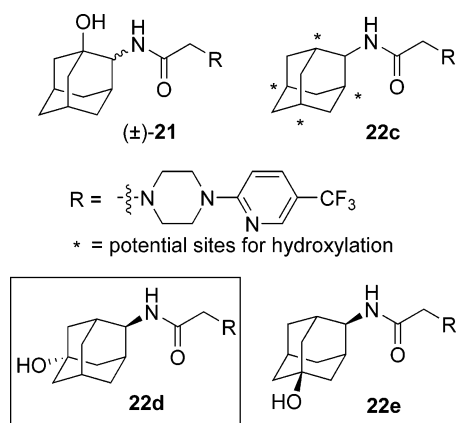
<sup>a</sup> Reagents and conditions: (a) catalytic 48% aqueous HBr, MeOH, reflux, 18 h, **25** (35%), **26** (37%); (b) DAST, CH<sub>2</sub>Cl<sub>2</sub>, -78 °C → 23 °C, 6 h, 63%; (c) NaH, MeI, toluene, microwave, 160 °C, 8 h, 21%; (d) DAST, CH<sub>2</sub>Cl<sub>2</sub>, -78 °C → 23 °C, 16 h, 5%.

**Figure 2.** High throughput screening hit **22a** and sites of HLM and MLM metabolism.**Table 1.** HSD1 Inhibition and Metabolism Studies for Unsubstituted Adamantanes **22b** and **22c**

	<b>22b</b>	<b>22c</b>
h-HSD1 K <sub>i</sub> <sup>a</sup>	5 nM	24 nM
m-HSD1 K <sub>i</sub> <sup>a</sup>	21 nM	51 nM
HEK IC <sub>50</sub> <sup>a</sup>	210 nM	190 nM
HLM CL <sub>int</sub>	35 L/h·kg	10 L/h·kg
MLM CL <sub>int</sub>	63 L/h·kg	142 L/h·kg

<sup>a</sup> Data is the geometric mean of at least two experiments.

methods (Scheme 1). 5-Acetoxy or 5-hydroxy-2-adamantanone **4** underwent reductive amination with ammonia to afford a 3:1 mixture of *E*- and *Z*-5-(acetoxy or hydroxy)-2-adamantamine **5a** and **5b**, respectively. Rhodium-catalyzed C–H insertion methodology<sup>36</sup> was utilized to prepare racemic 1-hydroxy-2-adamantamine (±)-**9** from 1-hydroxyadamantane **6**. Treatment of alcohol **6** with trichloroacetyl isocyanate followed by potassium carbonate provided the carbamate **7**.<sup>37</sup> Carbamate **7** was converted to the adamantyl oxazolidinone (±)-**8** by reaction with (diacetoxyiodo)benzene, magnesium oxide, and rhodium(II) acetate dimer dihydrate. Potassium hydroxide mediated oxazolidinone ring opening provided (±)-**9**.

**Figure 3.** Adamantane bridgehead oxidative metabolites of **22c**.

2,5,7-Trisubstituted adamantanes were prepared from simple adamantane precursors (Scheme 2). Preparation of *meso*-6-amino-adamantane-1,3-diol **13** from 2-aminoadamantane **10** began with acylation and bridgehead bromination to afford dibromo-acetamide **11**. Silver-promoted solvolysis of the bromides provided diol **12**, and acidic acetamide cleavage completed the preparation of **13**. 9-Amino-7-methylene-bicyclo[3.3.1]nonan-3-one **17** was prepared from 2-adamantanone **14**. Conversion of the ketone moiety in **14** to the homologated nitrile by reaction with *p*-toluenesulfonylmethyl isocyanide (TosMIC), followed by acidic hydrolysis and dibromination afforded the 5,7-dibromo-2-adamantane carboxylate **15**. Curtius reaction of the carboxylic acid **15** yielded the protected amine **16**. Deprotection and base-mediated adamantane ring opening provided **17**.

Side chain acid **19** was prepared from 5-trifluoromethyl-pyridin-2-yl piperazine **18** in three straightforward steps (Scheme 3). Alkylation of the piperazine **18** with methyl 2-bromopropionate, subsequent alkylation with methyl iodide, and ester hydrolysis afforded **19**.

Typical inhibitor and/or advanced core syntheses were performed by an acylation and amine alkylation sequence (Scheme 4). 2-Adamantamines **5a**, (±)-**9**, **10**, and **13** were converted to 2-(halo-acetyl-amino) adamantanes by reactions with 2-halo-acyl halides. Subsequent halide displacement by secondary amines afforded inhibitors and useful intermediates for further modification (**21** and **22a–g**, respectively). The *E*-

**Table 2.** HSD Inhibition, Selectivity, and Metabolism for Hydroxy- and Fluoro-Bridgehead Substituted Inhibitors

compd	substituent	h-HSD1 $K_i^a$ (nM)	h-HSD2 $IC_{50}^a$ (nM)	m-HSD1 $K_i^a$ (nM)	m-HSD2 $IC_{50}^a$ (nM)	HEK $IC_{50}^a$ (nM)	HLM $CL_{int}$ (L/h·kg)	MLM $CL_{int}$ (L/h·kg)
(±)- <b>21</b>		180	> 100 000	110	> 100 000	> 10 000	13	308
<b>22d</b>	R <sup>1</sup> = OH; R <sup>2</sup> = H	8	> 100 000	34	> 100 000	130	1	41
<b>22e</b>	R <sup>1</sup> = H; R <sup>2</sup> = OH	67	> 100 000	300	> 100 000	> 15 000	11	65
<b>27a</b>	R <sup>1</sup> = F; R <sup>2</sup> = H	32	> 20 000	120	> 100 000	550	2	136
<b>27b</b>	R <sup>1</sup> = H; R <sup>2</sup> = F	26	> 100 000	110	> 100 000	450	14	< 6

<sup>a</sup> Data is the geometric mean of at least two experiments.

**Table 3.** HSD Inhibition, Selectivity, and Metabolism of Substituted Acetamides **22d**, (±)-**22f**, and **23**

	<b>22d</b>	(±)- <b>22f</b>	<b>23</b>
h-HSD1 $K_i^a$ (nM)	8	5	8
h-HSD2 $IC_{50}^a$ (nM)	> 100 000	> 100 000	> 100 000
m-HSD1 $K_i^a$ (nM)	34	15	8
m-HSD2 $IC_{50}^a$ (nM)	> 100 000	> 100 000	> 100 000
HEK $IC_{50}^a$ (nM)	130	29	46
HLM $CL_{int}$ (L/h·kg)	1	3	6
MLM $CL_{int}$ (L/h·kg)	41	7	130

<sup>a</sup> Data is the geometric mean of at least two experiments.

**Table 4.** HSD1 Inhibition and Metabolism of Disubstituted Adamantane HSD1 Inhibitors

compd	h-HSD1 $K_i^a$ (nM)	m-HSD1 $K_i^a$ (nM)	HEK $IC_{50}^a$ (nM)	HLM $CL_{int}$ (L/h·kg)	MLM $CL_{int}$ (L/h·kg)
(±)- <b>22g</b>	62	4100	2100	< 1	< 6
<b>25</b>	10	470	430	< 1	23
<b>26</b>	6	180	110	< 1	60
(±)- <b>27c</b>	6	18	46	3	11
(±)- <b>27d</b>	12	33	120	< 1	14
(±)- <b>27e</b>	46	910	3400	1	56

<sup>a</sup> The data are the geometric mean of at least two experiments.

and *Z*-*meso*-isomers **22d–f** were separated by conventional chromatography, and their stereochemistry was assigned by the characteristic <sup>1</sup>H NMR relative chemical shift of the proton on the adamantyl C2 carbon.<sup>38</sup> The assignment of (±)-**22f** was confirmed crystallographically. The enantiomeric mixture (±)-**22f** was separated by reversed-phase chromatography on a chiral column.

A mixture of the *E*- and *Z*-5-hydroxy-2-adamantamine **5b** was coupled with acid **19** to provide the pure *E*-isomer **23**, after chromatographic separation from the *Z*-isomer (Scheme 5). Coupling with amino-enone **17** to provide amide **24** occurred similarly.

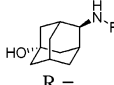
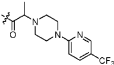
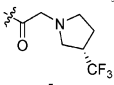
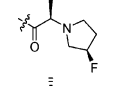
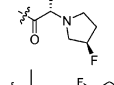
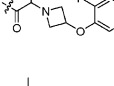
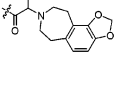
Two trisubstituted adamantane inhibitors were prepared, and modifications of several inhibitors were also conducted (Scheme 6). *meso*-Diol **25** and an *E/Z*-mixture of methoxy hydroxy adamantantyl **26** were obtained from the preceded ring closure reaction of enone **24** in refluxing methanol with catalytic aqueous hydrobromic acid.<sup>39</sup> *E*- and *Z*-5-Hydroxy-2-acetylaminoadmantanes **22d** and **22e** were converted to the corresponding *E*- and *Z*-5-fluoro **27a** and **27b**, respectively, with (diethylamino)sulfur trifluoride (DAST) in moderate yield.<sup>40</sup> Racemic *E*-5-hydroxy-2-propionylamino adamantane (±)-**22f** was converted to the 5-methoxy analog (±)-**27c** by Williamson ether synthesis. Treatment of 5,7-dihydroxy-2-propionylamino adamantyl (±)-**22g** with DAST afforded the chromatographically separable *E*- and *Z*-5-fluoro-7-hydroxy (±)-**27d** and (±)-**27e** in low yield.

**In Vitro and Ex Vivo Assays.** Inhibition of 11 $\beta$ -HSD1 enzymatic activity was assessed by a scintillation proximity assay (SPA). Crude lysates with truncated human, mouse, and rat 11 $\beta$ -HSD1 were incubated with the substrate, <sup>3</sup>H-cortisone, and the cofactor, NADPH. The radioactive cortisol generated was quantified in the absence and presence of inhibitors. Similar assays were developed for human, mouse, and rat 11 $\beta$ -HSD2 to assess the selectivity of compounds for 11 $\beta$ -HSD1. Cellular activity of the compounds was evaluated in HEK293 cells overexpressing human 11 $\beta$ -HSD1. The ability of the compounds to inhibit cortisone to cortisol conversion was measured in a fluorescent polarization immuno-assay (FPIA). The metabolic stability of compounds was evaluated in the presence of human, mouse, and rat liver microsomes. The parent remaining in the incubation mixture was measured by LC/MS, the *in vitro* metabolic half-life of substrate depletion was determined, and the half-life was converted into its hepatic intrinsic clearance. The effect and duration of orally dosed compound on murine target tissues (liver, adipose, and brain) was evaluated by an *ex vivo* 11 $\beta$ -HSD1 assay. Periodically, tissues were removed, minced, and incubated with cortisone. The cortisol generated was measured by LC/MS, and the percent inhibition of 11 $\beta$ -HSD1 activity relative to vehicle-treated controls was measured.

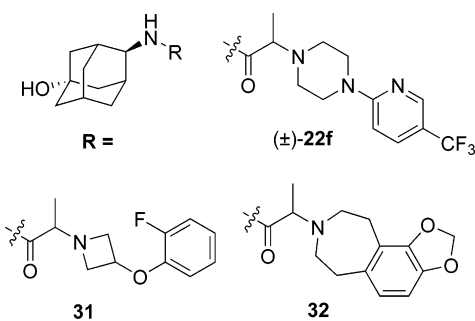
## Results and Discussion

A high throughput screen was conducted to identify potent and selective human 11 $\beta$ -hydroxysteroid dehydrogenase type 1 inhibitors. Adamantane **22a** (Figure 2) was identified and selected for hit to lead optimization as a result of its dual human and murine HSD1 potency, HSD2 selectivity, and cellular potency.<sup>41</sup> A similar profile was observed in a number of adamantane-containing hits. Adamantane-containing compounds have been shown to cross cell membranes and penetrate tissues effectively,<sup>40,42</sup> both of which are important for HSD1 inhibitors.

**Table 5.** HSD Inhibition, Selectivity, and Metabolism of **28** to **32**

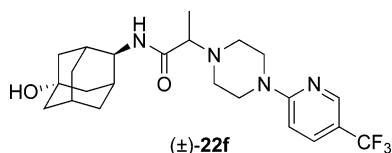
 R =	Compound	h-HSD1 $K_i$ (nM) <sup>a</sup>	h-HSD2 $IC_{50}$ (nM) <sup>a</sup>	m-HSD1 $K_i$ (nM) <sup>a</sup>	m-HSD2 $IC_{50}$ (nM) <sup>a</sup>	HEK $IC_{50}$ (nM) <sup>a</sup>	HLM $Cl_{int}$ (L/h·kg)	MLM $Cl_{int}$ (L/h·kg)
	(±)- <b>22f</b>	5	>100,000	15	>100,000	29	3	7
	<b>28</b>	3	>100,000	2	>100,000	35	< 1	60
	<b>29</b>	12	>100,000	9	>100,000	180	< 1	< 6
	<b>30</b>	21	>100,000	24	>100,000	450	< 1	< 6
	<b>31</b>	5	56,000	7	>100,000	71	< 1	23
	<b>32</b>	4	62,000	5	>100,000	21	2	20

<sup>a</sup> The data are the geometric mean of at least two experiments.

**Table 6.** Mouse Pharmacokinetic Data for (±)-**22f**, **31**, and **32**

compd	IV dose <sup>a</sup> (10 mg/kg)			oral dose <sup>a</sup> (10 mg/kg)		
	$t_{1/2}$ (h)	$V_{ss}$ (L/kg)	CL <sub>p</sub> (L/hr·kg)	$t_{1/2}$ (h)	AUC (ug/hr·mL)	$F$ (%)
(±)- <b>22f</b>	0.4	1.6	3.3	1.0	1.9	65
<b>31</b>	0.3	1.2	7.2	1.0	0.8	58
<b>32</b>	0.5	2.7	9.3	4.2	0.2	19

<sup>a</sup> Mean values ( $n = 3$ ) from nine mice for IV dosing and eight mice for oral dosing.

**Table 7.** *Ex Vivo* Mouse Study of (±)-**22f**<sup>a</sup>

liver <sup>b</sup>		adipose <sup>b</sup>		brain <sup>b</sup>	
1 h	7 h	1 h	7 h	1 h	7 h
36 ± 4	9 ± 15	51 ± 13	16 ± 20	37 ± 4	25 ± 5

<sup>a</sup> Oral dose, 30 mg/kg. <sup>b</sup> Values are % inhibition ± % SEM ( $n = 3$ ) within specified tissue at specified time.

However, adamantanes also typically have poor metabolic stability,<sup>43</sup> and both human and mouse microsomal metabolism studies on **22a** revealed significant liability with the formation of multiple metabolites. Further evaluation of the metabolism revealed three major metabolic events. Based on mass spectral

**Table 8.** HSD1 Inhibition and Metabolism of the *S*- and *R*-Enantiomers of (±)-**22f**<sup>a</sup>

compd	h-HSD1 $K_i$ <sup>a</sup> (nM)	m-HSD1 $K_i$ <sup>a</sup> (nM)	HEK $IC_{50}$ <sup>a</sup> (nM)	HLM $Cl_{int}$ (L/h·kg)	MLM $Cl_{int}$ (L/h·kg)
(±)- <b>22f</b>	5	15	29	3	7
( <i>S</i> )- <b>22f</b>	7	260	36	2	16
( <i>R</i> )- <b>22f</b>	4	5	26	1	< 6

<sup>a</sup> Data is the geometric mean of at least two experiments.

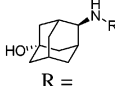
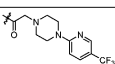
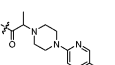
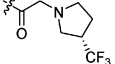
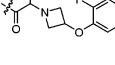
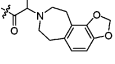
fragmentation patterns, aryl ring oxidation, adamantane oxidation, and *N*-piperazine dealkylation metabolites were identified.

The predicted site of aryl ring hydroxylation of **22a** was the position para to the piperazine ring. To overcome this liability, substituted analogs such as **22b** were evaluated and demonstrated improved metabolic stability (Table 1). Further investigation of the microsomal metabolism of **22b** revealed multiple metabolites, of which the predominant metabolite in both species was identical and the result of oxidation (M+16). Metabolite identification indicated that the hydroxylation occurred primarily on the adamantane ring. These studies also revealed a second common, minor, doubly hydroxylated adamantane metabolite (M + 32) but no triply hydroxylated metabolites. Another related analog is trifluoromethylpyridine **22c**, which demonstrated greater metabolic stability than **22b** in human liver microsomes. Furthermore, **22c** was metabolized to one predominant adamantane oxidative metabolite (M + 16) and, therefore, was attractive for additional modification to reduce metabolism. Compound **22c** also retained reasonable potency against HSD1.

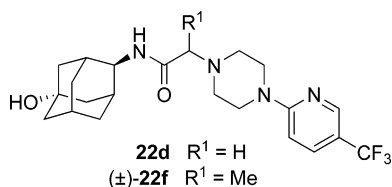
Precedent indicated the primary metabolite likely resulted from hydroxylation at a bridgehead carbon. Therefore, the bridgehead hydroxy-adamantyl analogs of **22c** (Figure 3) were prepared in the form of a racemic mixture (±)-**21** of the adjacent bridgehead analogs and the *meso-E*- and *Z*-distal bridgehead analogs **22d** and **22e**, respectively. Parallel and coelution HPLC studies of the metabolite mixture from **22c** with each of the hydroxy analogs (±)-**21**, **22d**, and **22e** indicated that the major metabolite of **22c** was the *E*-isomer **22d**.

Because fluorine substitution has been used to block adamantane metabolism, the distal bridgehead *E*- and *Z*-fluoro **27a** and **27b**, respectively, were also prepared. The hydroxy and fluoro analogs were evaluated for metabolic stability and

**Table 9.** Rat HSD, Cellular, and Metabolism Data for **22d**, ( $\pm$ )-**22f**, **28**, **31**, and **32**

 R =	Compound	r-HSD1 $K_i$ (nM) <sup>a</sup>	r-HSD2 $IC_{50}$ (nM) <sup>a</sup>	HEK $IC_{50}$ (nM) <sup>a</sup>	HLM $Cl_{int}$ (L/h·kg)	RLM $Cl_{int}$ (L/h·kg)
	<b>22d</b>	6	>100,000	130	1	< 3
	( $\pm$ )- <b>22f</b>	4	>100,000	29	3	5
	<b>28</b>	3	>100,000	35	< 1	28
	<b>31</b>	52	>100,000	71	< 1	4
	<b>32</b>	13	>100,000	21	2	34

<sup>a</sup> Data is the geometric mean of at least two experiments.

**Table 10.** Rat Pharmacokinetic Data for **22d** and ( $\pm$ )-**22f**

compd	IV dose <sup>a</sup> (5 mg/kg)			oral dose <sup>a</sup> (5 mg/kg)		
	$t_{1/2}$ (h)	$V_{ss}$ (L/kg)	CLp (L/hr·kg)	$t_{1/2}$ (h)	AUC (ug/h·mL)	$F$ (%)
<b>22d</b>	1.4	2.2	1.4	1.3	2.4	65
( $\pm$ )- <b>22f</b>	1.0	1.0	2.0	1.6	1.0	37

<sup>a</sup> Mean values ( $n = 3$ ) from three rats for IV dosing and three rats for oral dosing.

potency (Table 2). Of these compounds, the *meso-E*-hydroxy metabolite **22d** had the best profile. It was the most stable in the presence of HLM and the second most stable in the presence of MLM. Fortunately, the stability of **22d** was accompanied by potency and selectivity across species. Compound **22d** was assessed in >50 receptor binding assays and at concentrations <1  $\mu$ M, and no significant activity was detected.<sup>44</sup>

Interestingly, of the fluorinated analogs, the *Z*-isomer **27b** was more potent and more stable in the presence of MLM, but less stable in the presence of HLM. This suggested the potential for a beneficial complementarity between the *Z*-fluoro and the *E*-hydroxy substitutions. Other substitutions were also attempted, such as chloro, methyl, and methoxy, but all resulting analogs were rapidly metabolized (data not shown). This indicated a polar moiety, such as the hydroxy group, was necessary for stability.

To augment the metabolic stability gains achieved by modification of the aromatic and adamantane groups, the third and last site of initial metabolism of **22a** (*N*-dealkylation at the acetamide methylene linkage) was studied. Mono- and bis-substitution of the acetamide carbon linkage indicated that for potency small alkyl groups like methyl were preferred (*data not shown*). The *E*-hydroxy monomethyl ( $\pm$ )-**22f** and the *E*-hydroxy geminal dimethyl **23** combined the metabolic stabilizing effect of the *E*-hydroxy adamantane and methylene substitution. Both maintained reasonable h-HSD1 potency and

improved m-HSD1 and cellular potency (Table 3). While the monomethyl substitution of ( $\pm$ )-**22f** improved mouse stability and maintained human stability, the dimethyl substitution of **23** resulted in decreased metabolic stability in both mouse and human microsomes.

Additional adamantane metabolic stability improvements were pursued due to the results of the initial metabolism study of **22a**. In particular, the presence of a doubly hydroxylated adamantane metabolite of **22b** and the lack of a triply hydroxylated metabolite indicated that dihydroxylated compounds would be stable. Further studies on the primary site of hydroxylation suggested the secondary metabolite had undergone hydroxylation at the remaining distal bridgehead carbon to give a 2,5,7-trisubstituted adamantane. Dihydroxy analogs with mono- and gem-dimethyl acetamide substitution ( $\pm$ )-**22g** and **25**, respectively, did demonstrate improved stability in the presence of HLM and MLM. However, the human and mouse enzymatic activity and cellular potency of these analogs deteriorated relative to their monohydroxy equivalents. The hydroxy methoxy adamantyl *E/Z*-mixture **26** also showed improvements in human and mouse stability at the expense of mouse and cellular activity (detrimental effects were also observed for the simple methoxy analog of ( $\pm$ )-**22f**, ( $\pm$ )-**27c**). In a final attempt to improve the metabolic profile of this series, trisubstituted fluoro-hydroxy-*E*- and -*Z*-isomers ( $\pm$ )-**27d** and ( $\pm$ )-**27e**, respectively, were evaluated (Table 4). However, neither ( $\pm$ )-**27d** nor ( $\pm$ )-**27e** proved superior with only their human microsomal stability improved relative to ( $\pm$ )-**22f**. Although additional substitution at the 7-position with either a polar or nonpolar group maintained or improved HLM stability, no clear trend emerged for mouse microsomal stability. The 7-substitution did consistently and negatively impact both enzymatic and cellular potency with a few exceptions. The balanced improvement to stability and increased cellular activity achieved in the *E*-5-hydroxy adamantane of ( $\pm$ )-**22f** indicated the importance of this substitution pattern and the necessity for polarity.

With an understanding of the adamantane metabolism SAR in hand, we sought to identify a structurally diverse set of potent inhibitors. The *E*-5-hydroxy-2-aminoadamantane was held constant and acetamide substitution was varied. Five of the best compounds are reported in Table 5. Pyrrolidines **28**, **29**, and **30** have good profiles, but have decreased metabolic stability or cellular potency.

The pharmacokinetic profiles of ( $\pm$ )-**22f**, **31**, and **32** were evaluated *in vivo* in mice (Table 6). In accordance with their predicted metabolic stability, ( $\pm$ )-**22f** achieved the highest plasma concentrations. However, the clearance was still high, with a half-life of 1 h. The moderate to large volumes of distribution predicted good to excellent intracellular tissue penetration.

Because ( $\pm$ )-**22f** demonstrated the most favorable pharmacokinetic profile in this group, its 11 $\beta$ -HSD1 activity following oral dosing (30 mg/kg) was evaluated in a mouse *ex vivo* study using liver, adipose, and brain tissue at 1 and 7 h post-dose (Table 7). At 1 h, modest inhibition,  $\geq 36 \pm 4\%$ , was observed in all three tissues, while this inhibitory activity was either absent or declining by 7 h. These data indicated the identification of ( $\pm$ )-**22f** as a potent, selective, short-acting inhibitor, similar to other reported compounds used in proof of principle rodent studies.

To determine whether the dose potency of ( $\pm$ )-**22f** could be increased, the pure enantiomers were evaluated for HSD1 inhibition and metabolism (Table 8). Enantiomer (**R**)-**22f** was found to be more potent and stable. Thus, we hypothesize that dosing with pure (**R**)-**22f** should result in improved dose potency (greater exposure) than with the mixture.

The inhibitory activity of **22d**, ( $\pm$ )-**22f**, **28**, **31**, and **32** were also evaluated against rat 11 $\beta$ -HSD1, 11 $\beta$ -HSD2, and liver microsomes (r-HSD1, r-HSD2, and RLM) to determine if these inhibitors would be effective in rat models (Table 9). Although the rank order changed, all compounds were potent against r-HSD1, selective against r-HSD2, and trended toward greater stability in RLM than MLM. Interestingly, the *in vitro* profile for rat selectivity and metabolism for these compounds more closely paralleled the human potency and stability.

The pharmacokinetic profiles of **22d** and ( $\pm$ )-**22f** (Table 10), chosen for their potency and metabolic stability, were evaluated in rats. Consistent with microsomal stability data, **22d** and ( $\pm$ )-**22f** demonstrated high clearance values in rats. However, their moderate to high volume of distribution values provided for half-lives of over 1 h and suggested good tissue penetration. These improved pharmacokinetic properties in rats compared to mice, combined with the superior potency in rats, demonstrated the usefulness of HSD1 inhibitors, such as **22d**, as potent, selective, short-acting, HSD1 inhibitors, suitable for evaluation in rat models of MetS.

**Conclusion.** Starting from a rapidly metabolized adamantane inhibitor, a series of *E*-5-hydroxy-2-adamantamine 11 $\beta$ -HSD1 inhibitors with good cellular potency and improved microsomal stability were discovered. These inhibitors were potent against HSD1 and selective over HSD2 for multiples species, including human, mouse, and rat. One hour post-dose liver, adipose, and brain tissue 11 $\beta$ -HSD1 inhibition was confirmed in a murine *ex vivo* activity assay with ( $\pm$ )-**22f**. Profiling of these compounds in rodents indicated moderate to large volumes of distribution (associated with tissue and intracellular penetration), short half-lives. A clear pharmacokinetic difference was discovered between mice and rats with greater exposure in rats, particularly with **22d**. To further improve metabolic stability, desirable for sustained inhibition of 11 $\beta$ -HSD1 and akin to mini-pump administration of **2**, a second substituent was placed on the adamantane to give 5,7-disubstituted 2-adamantamines. This 7-substitution generally provided greater stability; however, it often decreased enzymatic potency and consistently decreased cellular potency. A single polar functional group in the *E*-5-position afforded inhibitors with the best combination of stability, potency, selectivity, and species generality. These results indicate that, when the polar substituent in the *E*-5-

position is a hydroxyl group, adamantane metabolic stabilization sufficient to obtain *short-acting*, potent, and selective 11 $\beta$ -HSD1 inhibitors has been achieved.

## Experimental Section

**Compound Preparation.** Unless otherwise specified, all solvents and reagents were obtained from commercial suppliers and used without further purification. All reactions were performed under a nitrogen atmosphere unless specifically noted. Normal-phase flash chromatography was done using Merck silica gel 60 (230–400 mesh) from E.M. Science or was performed on a hybrid system employing Gilson components and Biotage prepacked columns. Reversed-phase chromatography was performed using a Gilson 215 solvent handler-driven HPLC system (CH<sub>3</sub>CN/0.1% TFA in H<sub>2</sub>O or CH<sub>3</sub>CN/NH<sub>4</sub>OAc in H<sub>2</sub>O) on a YMC ODS Guardpak column. Analytical LC-MS was performed on a Finnigan Navigator mass spectrometer and Agilent 1100 HPLC system running Xcalibur 1.2 and Open-Access 1.3 software. The mass spectrometer was operated under positive APCI ionization conditions. The HPLC system comprised an Agilent Quaternary pump, degasser, column compartment, autosampler, and diode-array detector, with a Sedere Sedex 75 evaporative light-scattering detector. The column used was a Phenomenex Luna Combi-HTS C8(2) 5  $\mu$ m 100 Å (2.1 mm  $\times$  30 mm). A gradient of 10–100% acetonitrile (A) and 0.1% trifluoroacetic acid in water (B; or alternatively 0.01% ammonium acetate in water) was used, at a flow rate of 1.5 mL/min (0–0.1 min 10% A, 0.1–3.1 min 10–100% A, 3.1–3.9 min 100–10% A, 3.9–4.0 min 100–10% A). <sup>1</sup>H NMR spectra were recorded at 300 and 500 MHz; all values are referenced to tetramethylsilane as internal standard and are reported as shift (multiplicity, coupling constants, proton count). Mass spectral analysis is accomplished using atmospheric pressure chemical ionization (APCI), electrospray ionization (ESI), or direct chemical ionization (DCI) techniques. All elemental analyses are consistent with theoretical values to within  $\pm 0.4\%$ , unless indicated.

***E*- and *Z*-Acetic Acid 2-Amino-adamantan-5-yl Ester (5a).** A solution of 5-hydroxy-2-adamantanone (2.6 g, 16 mmol) in CH<sub>2</sub>-Cl<sub>2</sub> (50 mL) was treated with DMAP (2.1 g, 17 mmol) and acetic anhydride (2.3 mL, 23 mmol) and stirred at 50 °C overnight. The solvent was removed under reduced pressure, and the residue was partitioned between water and EtOAc. The aqueous layer was extracted twice with EtOAc. The combined organic extracts were washed with water, dried (MgSO<sub>4</sub>), and filtered. The filtrate was concentrated under reduced pressure to provide acetic acid 2-oxo-adamantan-5-yl ester as an off-white solid (3.1 g, 87%).

A solution of the ester (3.1 g, 15 mmol) and 4 Å molecular sieves (1 g) in methanolic ammonia (7 N, 50 mL) was stirred at room temperature overnight. The reaction mixture was cooled in an ice bath, treated portionwise with sodium borohydride (2.3 g, 60 mmol), and stirred at room temperature for 2 h. The suspension was filtered and concentrated under reduced pressure. The residue was dissolved in CH<sub>2</sub>Cl<sub>2</sub> (50 mL) and acidified with 1 N hydrochloric acid solution to pH = 3. The two layers were separated. The aqueous layer was treated with 2 N sodium hydroxide to pH = 12 and extracted three times with 4:1 THF/CH<sub>2</sub>Cl<sub>2</sub>. The combined organic extracts were dried (MgSO<sub>4</sub>) and filtered. The filtrate was concentrated under reduced pressure to provide a 3:1 *E/Z* mixture of esters (**5a**) as a white solid (1.8 g, 58%).

***E*- and *Z*-5-Hydroxy-2-adamantamine (5b).** A solution of 5-hydroxy-2-adamantanone (10 g, 60 mmol) and 4 Å molecular sieves (5 g) in methanolic ammonia (7 N, 100 mL) was stirred at room temperature overnight. The reaction mixture was cooled in an ice bath, treated by the portionwise addition of sodium borohydride (9.1 g, 240 mmol), and stirred at room temperature for 2 h. The suspension was filtered and concentrated under reduced pressure. The residue was dissolved in CH<sub>2</sub>Cl<sub>2</sub> (100 mL) and acidified with 1 N hydrochloric acid solution to pH = 3. The two layers were separated. The aqueous layer was treated with 2 N sodium hydroxide solution to pH = 12 and extracted three times with 4:1 THF/CH<sub>2</sub>Cl<sub>2</sub>. The combined organic extracts were dried



(MgSO<sub>4</sub>) and filtered. The filtrate was concentrated under reduced pressure to provide a 3:1 *E/Z* mixture of aminoalcohols (**5b**) as a white solid (9.8 g, 98%).

**Carbamic Acid Adamantan-2-yl Ester (7).** A 0 °C solution of adamant-1-ol (1.5 g, 10 mmol) in CH<sub>2</sub>Cl<sub>2</sub> (50 mL) was treated with trichloroacetylisocyanate (1.4 mL, 12 mmol). The reaction mixture was stirred at room temperature for 2 h and concentrated under reduced pressure. The residue was dissolved in MeOH (20 mL) and treated with a saturated potassium carbonate solution (30 mL). The reaction mixture was stirred at 50 °C for 16 h; the MeOH was removed under reduced pressure; and the white precipitate was filtered and washed with water. Drying overnight in a vacuum oven provided the carbamate (**7**) as a white powder (1.7 g, 87%). MS (APCI) *m/z* 196 (M + H)<sup>+</sup>.

**Adamantane-oxazolidinone (±)-8.** A solution of carbamic acid adamantan-2-yl ester (0.59 g, 3.0 mmol) in CH<sub>2</sub>Cl<sub>2</sub> was treated with iodobenzenediacetate (1.3 g, 4.2 mmol), magnesium oxide (0.28 g, 6.9 mmol), and rhodium diacetate dimer (0.13 g, 0.29 mmol). The reaction mixture was stirred at 50 °C for 4 h and filtered. The filtrate was concentrated under reduced pressure and purified by flash column chromatography on silica gel with 10% acetone in hexane to provide the oxazolidinone (±)-**8** as a white solid (0.40 g, 69%). <sup>1</sup>H NMR (300 MHz, CDCl<sub>3</sub>)  $\delta$  4.8 (s, 1H), 3.66 (s, 1H), 2.29 (s, 2H), 2.14 (m, 4H), 1.89–1.75 (m, 2H), 1.72 (d, 2H), 1.68–1.61 (m, 3H); MS (APCI) *m/z* 194 (M + H)<sup>+</sup>.

**1-Amino-adamantan-2-ol (±)-9.** A solution of adamantane-oxazolidinone (0.40 g, 2.1 mmol) in dioxane (1 mL) was treated with 5 N potassium hydroxide solution (5 mL) and stirred at 70 °C overnight. The dioxane was removed under reduced pressure, and the residue was partitioned between brine and THF/CH<sub>2</sub>Cl<sub>2</sub> 4:1. The layers were separated, and the aqueous layer was extracted twice with THF/CH<sub>2</sub>Cl<sub>2</sub> 4:1. The combined organic extracts were washed with brine, dried (MgSO<sub>4</sub>), and filtered. The filtrate was concentrated under reduced pressure to provide the aminoalcohol (±)-**9** as a white solid (0.30 g, 87%).

**N-Adamantan-2-yl Acetamide.** A solution of 2-adamantanamine hydrochloride (5.0 g, 27 mmol) in anhydrous pyridine (30 mL) was treated with acetic anhydride (3.0 mL, 32 mmol) and stirred at room temperature overnight. The reaction mixture was diluted with EtOAc and washed with water, 1 N phosphoric acid solution, and brine. The organic layer was dried (Na<sub>2</sub>SO<sub>4</sub>), filtered, and concentrated under reduced pressure. The residue was purified by flash column chromatography on silica gel with 40–50% EtOAc in hexane to provide the acetamide as a white solid (4.0 g, 75%). <sup>1</sup>H NMR (300 MHz, CDCl<sub>3</sub>)  $\delta$  5.74 (m, 1H), 4.04 (m, 1H), 2.01 (s, 3H), 2.00–1.60 (m, 14H); MS (DCI) *m/z* 194 (M + H)<sup>+</sup>.

**N-(5,7-Dibromoadamantan-2-yl)acetamide (11).** Over a period of 30 min, *N*-adamantan-2-yl acetamide (2.0 g, 10 mmol) was added portionwise to a flask equipped with a reflux condenser and charged with bromine (10 mL, 20 mmol) and aluminum bromide (0.59 g, 2.2 mmol). The reaction mixture was stirred at 90 °C for 4 days. After 4 days, additional bromine (10 mL, 20 mmol) and aluminum bromide (0.59 g, 2.2 mmol) were added. The reaction was continued for three more days at 90 °C. The reaction mixture was cooled in an ice bath, and ice water (100 mL) and CH<sub>2</sub>Cl<sub>2</sub> (100 mL) were added. This mixture was quenched by slow addition of saturated sodium bisulfite solution, followed by further dilution with CH<sub>2</sub>Cl<sub>2</sub> (100 mL). The organic layer was separated, washed with water and brine, dried (Na<sub>2</sub>SO<sub>4</sub>), and filtered. The filtrate was concentrated under reduced pressure and purified by flash column chromatography on silica gel with 0–70% ethyl acetate in hexane to provide the dibromide (**11**; 0.76 g, 21%). <sup>1</sup>H NMR (300 MHz, CDCl<sub>3</sub>)  $\delta$  5.53 (m, 1H), 4.04 (m, 1H), 2.87 (bs, 2H), 2.50–2.05 (m, 9H), 2.02 (s, 3H), 1.83 (m, 1H); MS (DCI) *m/z* 352 (M + H)<sup>+</sup>.

**N-(5,7-Dihydroxyadamantane-2-yl)acetamide (12).** *N*-(5,7-Dibromoadamantan-2-yl)acetamide (0.76 g, 2.2 mmol) and silver sulfate (1.5 g, 4.8 mmol) were treated with concentrated sulfuric acid (5 mL), and the reaction mixture was heated at 80 °C for 2 h. The reaction mixture was filtered, and the solids were washed with water. The filtrate was neutralized with solid potassium hydroxide

and filtered, and the solids were washed with water and methanol. The filtrate was concentrated under reduced pressure, and the resultant solids were triturated with MeOH. The heterogeneous mixture was filtered, and the filtrate was concentrated under reduced pressure. The concentrate was purified by flash column chromatography on silica gel with 10–20% MeOH in CH<sub>2</sub>Cl<sub>2</sub> to provide the diol (**12**; 0.34 g, 70%). <sup>1</sup>H NMR (300 MHz, DMSO-*d*<sub>6</sub>)  $\delta$  7.62 (m, 1H), 4.47 (s, 1H), 4.45 (s, 1H), 3.57 (m, 1H), 1.99 (m, 2H), 1.82 (s, 3H), 1.77 (m, 2H), 1.60–1.40 (m, 6H), 1.25 (m, 2H); MS (DCI) *m/z* 226 (M + H)<sup>+</sup>.

**6-Aminoadamantane-1,3-diol (13).** A solution of *N*-(5,7-dihydroxyadamantane-2-yl)acetamide (0.34 g, 1.5 mmol) in water (3 mL) was treated with 6 N hydrochloric acid solution (3 mL) and heated at 80 °C overnight. The reaction mixture was concentrated under reduced pressure, and the residue was treated with saturated sodium bicarbonate solution. The water was removed under reduced pressure, and the solid residue was triturated with MeOH. The heterogeneous mixture was filtered, and the solids were washed with MeOH. The filtrate was concentrated under reduced pressure to provide the aminodiol (**13**; 0.28 g, 100%). <sup>1</sup>H NMR (300 MHz, D<sub>2</sub>O)  $\delta$  3.34 (m, 1H), 2.38 (m, 2H), 1.80–1.65 (m, 8H), 1.59 (m, 2H); MS (DCI) *m/z* 184 (M + H)<sup>+</sup>.

**5,7-Dibromo-adamantane-2-carboxylic Acid (15).** A 0 °C solution of 2-adamantanone (7.2 g, 48 mmol) in DME (165 mL) and EtOH (5 mL) was treated with *p*-toluenesulfonylmethyl isocyanide (12 g, 62 mmol), followed by portionwise addition of solid *t*-BuOK (13 g, 120 mmol), maintaining the temperature below 10 °C. After the addition, the reaction mixture was stirred at room temperature for 30 min and then at 35–40 °C for 30 min. The heterogeneous reaction mixture was filtered, and the solids were washed with DME. The filtrate was concentrated, loaded to a short aluminum oxide column, and washed off with a 5:1 mixture of hexane/CH<sub>2</sub>Cl<sub>2</sub> (600 mL). The solution was concentrated to provide adamantane-2-carbonitrile as a white solid (7.5 g, 98%).

A solution of the nitrile (7.5 g, 47 mmol) in AcOH (22 mL) and 48% hydrobromic acid solution (90 mL) was stirred at 120 °C overnight. The reaction mixture was cooled in a refrigerator, filtered, washed with water, and dried in a vacuum oven overnight to provide adamantane-2-carboxylic acid as an off-white solid (5.4 g, 64%).

A vigorously stirred 0 °C solution of aluminum bromide (8.8 g, 33 mmol) and bromine (30 mL) was treated portionwise with the acid (5.4 g, 30 mmol). Upon completion of the addition, the ice bath was removed and the reaction mixture was warmed to room temperature and then slowly to 70 °C over 2 h. The reaction mixture was stirred at 70 °C overnight, cooled in an ice bath, and quenched carefully with a saturated sodium bisulfite solution. The resultant heterogeneous mixture was filtered and washed with water. The collected solid was dried in a vacuum oven overnight to provide **15** as a tan solid (7.5 g, 74%). <sup>1</sup>H NMR (500 MHz, DMSO-*d*<sub>6</sub>)  $\delta$  12.35 (s, 1H), 2.83 (s, 2H), 2.72 (s, 1H), 2.34–2.19 (m, 10H); MS (ESI) *m/z* 337 (M + H)<sup>+</sup>.

**9-Amino-7-methylene-bicyclo[3.3.1]nonan-3-one (17).** A room temperature solution of 5,7-dibromo-adamantane-2-carboxylic acid (340 mg, 1.0 mmol) in toluene (3 mL) was treated with diphenylphosphoryl azide (300 mg, 1.1 mmol) and triethylamine (150  $\mu$ L, 1.1 mmol) and stirred at reflux for 1 h. The reaction mixture was cooled to room temperature and concentrated under reduced pressure. The residue was dissolved in *t*-BuOH (1 mL) and refluxed for 24 h. Evaporation of the *t*-BuOH provided the crude (5,7-dibromo-adamantan-2-yl)-carbamic acid *tert*-butyl ester (**16**; 180 mg, 44%).

A solution of **16** (180 mg, 0.44 mmol) in dioxane (2 mL) was treated with 2 N sodium hydroxide solution (1 mL) and irradiated with microwaves in a Personal Chemistry Emrys Optimizer for 15 min at 180 °C. The dioxane was removed under reduced pressure. The residue was dissolved in CH<sub>2</sub>Cl<sub>2</sub>, dried (MgSO<sub>4</sub>), and concentrated to provide crude amino-enone (**17**; 69 mg, 95%).

**2-Methyl-2-[4-(5-trifluoromethyl-pyridin-2-yl)-piperazin-1-yl]-propionic Acid (19).** A solution of 1-(5-trifluoromethyl-pyridin-2-yl)-piperazine (0.90 g, 3.9 mmol) in MeOH (13 mL) and DIPEA (1.5 mL) was treated with 2-bromo-propionic acid methyl ester

(0.48 mL, 4.3 mmol) and stirred at 70 °C overnight. The MeOH was removed under reduced pressure, and the residue was purified by flash column chromatography on silica gel with 10–40% acetone in hexane to provide 2-[4-(5-trifluoromethyl-pyridin-2-yl)-piperazin-1-yl]-propionic acid methyl ester as a yellowish solid (1.2 g, 100%).

A solution of the ester (1.2 g, 3.9 mmol) in THF (3 mL) was added dropwise to a –65 °C solution of 1.8 N LDA (2.4 mL, 4.3 mmol) in THF (2 mL) and stirred for 1 h. Methyl iodide (0.49 mL, 7.9 mmol) was added, and the reaction mixture was slowly warmed to room temperature and stirred for 2 h. The reaction mixture was quenched with ice/water. The aqueous layer was extracted with EtOAc (3×). The combined organic extracts were washed with water, dried (MgSO<sub>4</sub>), filtered, and concentrated under reduced pressure. The residue was purified by flash column chromatography on silica gel with 10–30% acetone in hexane to provide 2-methyl-2-[4-(5-trifluoromethyl-pyridin-2-yl)-piperazin-1-yl]-propionic acid methyl ester as a yellowish solid (1.0 g, 81%).

A solution of the ester (1.0 g, 3.2 mmol) in dioxane (10 mL) was treated with 5 N potassium hydroxide solution (10 mL) and stirred at 60 °C for 4 h. The dioxane was removed under reduced pressure. The residue was neutralized with 1 N hydrochloric acid solution to pH = 7 and extracted three times with 4:1 THF/CH<sub>2</sub>-Cl<sub>2</sub>. The combined organic extracts were dried (MgSO<sub>4</sub>), filtered, and concentrated under reduced pressure to provide the acid (**19**) as a white solid (0.90 g, 90%).

**N-(1-Hydroxy-adamantan-2-yl)-2-[4-(5-trifluoromethyl-pyridin-2-yl)-piperazin-1-yl]-acetamide (21)**. A 0 °C solution of 1-amino-adamantan-2-ol (**5b**; 33 mg, 0.20 mmol) in CH<sub>2</sub>Cl<sub>2</sub> (1 mL) and DIPEA (0.1 mL) was treated with chloroacetyl chloride (0.020 mL, 0.25 mmol). The reaction mixture was stirred at room temperature for 2 h and concentrated under reduced pressure. The residue was purified by flash column chromatography on silica gel with 4:1 hexane/acetone to provide the 2-chloro-*N*-(2-hydroxy-adamantan-1-yl)-acetamide as a beige solid (41 mg, 85%).

A solution of the acetamide (41 mg, 0.17 mmol) in MeOH (1 mL) and DIPEA (0.1 mL) was treated with 1-(5-trifluoromethyl-pyridin-2-yl)-piperazine (46 mg, 0.20 mmol). The reaction mixture was stirred at 70 °C overnight. The MeOH was removed under reduced pressure. The residue was purified by reversed-phase HPLC to provide **21** (44 mg, 60%). <sup>1</sup>H NMR (300 MHz, CDCl<sub>3</sub>) δ 8.41 (d, *J* = 1.70 Hz, 1H), 7.66 (dd, *J* = 8.99, 2.54 Hz, 2H), 6.67 (d, *J* = 8.82 Hz, 1H), 4.00 (d, *J* = 8.14 Hz, 1H), 3.69 (s, 4H), 3.15 (s, 2H), 2.93 (d, *J* = 5.09 Hz, 1H), 2.70 (s, 4H), 2.06–2.18 (m, 3H), 1.72–1.87 (m, 4H), 1.63 (d, *J* = 3.73 Hz, 4H), 1.59 (s, 2H); MS (APCI) *m/z* 439 (M + H)<sup>+</sup>. Anal. (C<sub>22</sub>H<sub>29</sub>F<sub>3</sub>N<sub>4</sub>O<sub>2</sub>·1.1H<sub>2</sub>O) C, H, N.

**N-Adamantan-2-yl-2-chloro-acetamide**. A 0 °C suspension of 2-adamantanamine hydrochloride (1.8 g, 9.6 mmol) in CH<sub>2</sub>Cl<sub>2</sub> (30 mL) and DIPEA (3.5 mL, 20 mmol) was treated with chloroacetyl chloride (0.78 mL, 9.6 mmol). The reaction mixture was stirred at room temperature for 2 h and concentrated under reduced pressure. The residue was partitioned between water and EtOAc. The organic layer was washed with saturated sodium bicarbonate solution and water, dried (MgSO<sub>4</sub>), and filtered. The filtrate was concentrated under reduced pressure to provide the chloroacetamide as a dark tan solid (2.1 g, 92%). MS (DCI) *m/z* 228 (M + H)<sup>+</sup>.

**N-Adamantan-2-yl-2-[4-(3-cyano-pyridin-2-yl)-piperazin-1-yl]-acetamide (22a)**. A solution of 1-(2-cyanopyridyl)piperazine (680 mg, 3.6 mmol) and DIPEA (2 mL) in toluene (30 mL) was treated with the *N*-2-adamantyl-2-chloroacetamide (670 mg, 2.9 mmol) and heated at 60 °C overnight. The reaction mixture was cooled to room temperature and washed with saturated sodium bicarbonate solution. The organic layer was dried (Na<sub>2</sub>SO<sub>4</sub>) and concentrated. The residue was purified by flash column chromatography on silica gel with 20% EtOAc in hexanes to provide **22a** as a white solid (920 mg, 82%). <sup>1</sup>H NMR (300 MHz, DMSO-*d*<sub>6</sub>) δ 8.41 (dd, *J* = 4.8, 1.7 Hz, 1H), 8.08 (dd, *J* = 7.8, 2.0 Hz, 1H), 7.69 (br d, *J* = 7.8 Hz, 1H), 6.94 (dd, *J* = 7.5, 4.7 Hz, 1H), 3.88 (br d, *J* = 7.8 Hz, 1H), 3.62 (m, 4H), 3.04 (s, 2H), 2.63 (m, 4H), 1.79 (m, 12H), 1.57 (d, *J* = 12.5 Hz, 2H); MS (DCI) *m/z* 380 (M + H)<sup>+</sup>. Anal. (C<sub>22</sub>H<sub>29</sub>N<sub>5</sub>O·0.2H<sub>2</sub>O) C, H, N.

**N-Adamantan-2-yl-2-[4-(4-chloro-phenyl)-piperazin-1-yl]-acetamide (22b)**. A solution of *N*-adamantan-2-yl-2-chloro-acetamide (23 mg, 0.10 mmol) in MeOH (0.5 mL) and DIPEA (21 μL, 0.12 mmol) was treated with 1-(4-chlorophenyl)-piperazine (23 mg, 0.12 mmol) and stirred at 70 °C overnight. The MeOH was removed under reduced pressure. The residue was dissolved in CH<sub>2</sub>Cl<sub>2</sub>, washed twice with water, dried (MgSO<sub>4</sub>), and filtered. The filtrate was concentrated under reduced pressure and purified by reversed-phase HPLC to provide **22b** (26 mg, 65%). <sup>1</sup>H NMR (500 MHz, CDCl<sub>3</sub>) δ 7.70 (d, *J* = 8.11 Hz, 1H), 7.20–7.25 (m, 2H), 6.83–6.87 (m, 2H), 4.09 (d, *J* = 8.73 Hz, 1H), 3.17–3.24 (m, 4H), 3.09 (s, 2H), 2.70–2.76 (m, 4H), 1.91 (s, 2H), 1.83–1.88 (m, 6H), 1.71–1.78 (m, 4H), 1.65–1.70 (m, 2H); MS (APCI) *m/z* 388 (M + H)<sup>+</sup>. Anal. (C<sub>22</sub>H<sub>30</sub>ClN<sub>3</sub>O·0.5H<sub>2</sub>O) C, H, N.

**N-Adamantan-2-yl-2-[4-(5-trifluoromethyl-pyridin-2-yl)-piperazin-1-yl]-acetamide (22c)**. A solution of *N*-adamantan-2-yl-2-chloro-acetamide (23 mg, 0.10 mmol) in MeOH (0.5 mL) and DIPEA (21 μL, 0.12 mmol) was treated with 1-(5-trifluoromethyl-pyridin-2-yl)-piperazine (28 mg, 0.12 mmol) and stirred at 70 °C overnight. The MeOH was removed under reduced pressure. The residue was dissolved in CH<sub>2</sub>Cl<sub>2</sub>, washed twice with water, dried (MgSO<sub>4</sub>), and filtered. The filtrate was concentrated under reduced pressure and purified by reversed-phase HPLC to provide (**22c**) as a white solid (30 mg, 71%). <sup>1</sup>H NMR (500 MHz, CDCl<sub>3</sub>) δ 8.42 (s, 1H), 7.76 (s, 1H), 7.66 (dd, *J* = 8.89, 2.34 Hz, 1H), 6.67 (d, *J* = 9.04 Hz, 1H), 4.10 (d, *J* = 8.42 Hz, 1H), 3.75 (s, 4H), 3.20 (s, 2H), 2.79 (s, 3H), 1.92 (s, 8H), 1.75–1.68 (m, 6H); MS (APCI) *m/z* 423 (M + H)<sup>+</sup>. Anal. (C<sub>22</sub>H<sub>29</sub>F<sub>3</sub>N<sub>4</sub>O·0.65CF<sub>3</sub>CO<sub>2</sub>H) C, H, N.

**N-[(E)-5-Hydroxy-2-adamantyl]-2-[4-[5-(trifluoromethyl)pyridin-2-yl]piperazin-1-yl]acetamide (22d)**. A 0 °C solution of **5a** (1.8 g, 8.7 mmol) in CH<sub>2</sub>Cl<sub>2</sub> (30 mL) and DIPEA (1.7 mL, 10 mmol) was treated with chloroacetyl chloride (0.76 mL, 9.6 mmol). The reaction mixture was stirred at room temperature for 2 h and concentrated under reduced pressure. The residue was partitioned between water and EtOAc. The organic layer was washed with saturated aqueous sodium bicarbonate solution and water, dried (MgSO<sub>4</sub>), and filtered. The filtrate was concentrated under reduced pressure to provide a 2:1 *E/Z* mixture of acetic acid 2-(2-chloroacetyl-amino)-adamantan-5-yl esters as a dark beige solid (2.1 g, 84%).

A solution of the esters (2.1 g, 7.3 mmol) in MeOH (30 mL) and DIPEA (1.5 mL, 8.8 mmol) was treated with 1-(5-trifluoromethyl-pyridin-2-yl)-piperazine (2.0 g, 8.8 mmol) and stirred at 70 °C for 6 h. A saturated potassium carbonate solution (15 mL) was added to the reaction and stirred at 70 °C overnight. The MeOH was removed under reduced pressure. The residue was dissolved in CH<sub>2</sub>Cl<sub>2</sub>, washed twice with water, dried (MgSO<sub>4</sub>), and filtered. The filtrate was concentrated under reduced pressure to provide an off-white solid, which was purified by flash column chromatography on silica gel with 30–90% acetone in hexane to provide **22d** as a white solid (1.0 g, 46%). <sup>1</sup>H NMR (300 MHz, CDCl<sub>3</sub>) δ 8.41 (s, 1H), 7.67 (dd, *J* = 2.1, 9.1 Hz, 1H), 7.6 (s, 1H), 6.67 (d, *J* = 9.1 Hz, 1H), 4.07 (d, *J* = 8.1 Hz, 1H), 3.69 (s, 4H), 3.1 (s, 2H), 2.68 (s, 4H), 2.12–2.17 (m, 3H), 1.91 (m, 2H), 1.79–1.75 (m, 4H), 1.67 (m, 2H), 1.57 (s, 1H), 1.36 (s, 1H); MS (APCI) *m/z* 439 (M + H)<sup>+</sup>. Anal. (C<sub>22</sub>H<sub>29</sub>F<sub>3</sub>N<sub>4</sub>O<sub>2</sub>·0.45H<sub>2</sub>O) C, H, N.

**N-[(Z)-5-Hydroxy-2-adamantyl]-2-[4-[5-(trifluoromethyl)pyridin-2-yl]piperazin-1-yl]acetamide (22e)**. Purification of the concentrated filtrate from the previous step by flash column chromatography on silica gel with 30–90% acetone in hexane provided (**22e**) as a white solid (0.50 g, 23%). <sup>1</sup>H NMR (300 MHz, CDCl<sub>3</sub>) δ 8.41 (s, 1H), 7.65 (dd, *J* = 2.7, 9.1 Hz, 1H), 7.6 (s, 1H), 6.65 (d, *J* = 9.1 Hz, 1H), 3.98 (d, *J* = 8.5 Hz, 1H), 3.69 (s, 4H), 3.09 (s, 2H), 2.67 (s, 4H), 2.19–2.15 (m, 3H), 1.79–1.38 (m, 10H); MS (APCI) *m/z* 439 (M + H)<sup>+</sup>. Anal. (C<sub>22</sub>H<sub>29</sub>F<sub>3</sub>N<sub>4</sub>O<sub>2</sub>) C, H, N.

**N-[(E)-5-Hydroxy-2-adamantyl]-2-[4-[5-(trifluoromethyl)pyridin-2-yl]piperazin-1-yl]propionamide (22f)**. A 0 °C solution of **5a** (0.54 g, 2.6 mmol) in CH<sub>2</sub>Cl<sub>2</sub> (10 mL) and DIPEA (0.54 mL, 3.1 mmol) was treated with 2-bromopropionyl chloride (0.26 mL, 2.6 mmol). The reaction mixture was stirred at room temperature for 2 h and concentrated under reduced pressure. The residue was

partitioned between water and EtOAc. The organic layer was washed with saturated aqueous sodium bicarbonate solution and water, dried (MgSO<sub>4</sub>), and filtered. The filtrate was concentrated under reduced pressure to provide a 2:1 *E/Z* mixture of acetic acid 2-(2-bromo-propionylamino)-adamantan-5-yl esters as a dark beige solid (0.75 g, 71%).

A solution of the esters (0.75 g, 2.2 mmol) in MeOH (10 mL) and DIPEA (0.42 mL, 2.4 mmol) was treated with 1-(5-trifluoromethyl-pyridin-2-yl)-piperazine (0.55 g, 2.4 mmol) and stirred at 70 °C for 6 h. A saturated potassium carbonate solution (10 mL) was added to the reaction and stirred at 70 °C overnight. The MeOH was removed under reduced pressure. The residue was dissolved in CH<sub>2</sub>Cl<sub>2</sub>, washed twice with water, dried (MgSO<sub>4</sub>), and filtered. The filtrate was concentrated under reduced pressure to provide an off-white solid, which was purified by reversed-phase HPLC to provide **22f** as a white solid (500 mg, 53%). <sup>1</sup>H NMR (300 MHz, CDCl<sub>3</sub>)  $\delta$  8.41 (s, 1H), 7.65 (m, 2H), 6.67 (d, *J* = 8.8 Hz, 1H), 4.03 (d, *J* = 8.5 Hz, 1H), 3.69 (m, 4H), 3.15 (q, *J* = 7.1 Hz, 1H), 2.63 (m, 4H), 2.15 (m, 3H), 1.9 (m, 2H), 1.77 (m, 4H), 1.66 (m, 2H), 1.52 (s, 1H), 1.36 (s, 1H), 1.28 (d, *J* = 7.1 Hz, 3H); MS (APCI) *m/z* 453 (M + H)<sup>+</sup>. Anal. (C<sub>23</sub>H<sub>31</sub>F<sub>3</sub>N<sub>4</sub>O<sub>2</sub>·0.25H<sub>2</sub>O) C, H, N.

**2-Bromo-*N*-(5,7-dihydroxyadamantan-2-yl)propionamide.** A 0 °C solution of **13** (0.28 g, 1.5 mmol) in 1:1 saturated sodium bicarbonate solution/water (3 mL) was treated with 2-bromopropionyl chloride (0.17 mL, 1.7 mmol), stirred for 30 min, and warmed to room temperature overnight. An additional amount of 2-bromopropionyl chloride (0.085 mL, 0.84 mmol) was added. The reaction mixture was stirred at room temperature for 1 h and at 50 °C for 2 h. The solvents were removed under reduced pressure, and the residue was purified by flash column chromatography on silica gel with 5–10% MeOH in CH<sub>2</sub>Cl<sub>2</sub> to provide the bromide (0.17 g, 36%). <sup>1</sup>H NMR (500 MHz, DMSO-*d*<sub>6</sub>)  $\delta$  7.95 (d, *J* = 6 Hz, 1H), 4.72 (q, *J* = 7 Hz, 1H), 4.48 (m, 2H), 3.56 (m, 1H), 2.03 (m, 2H), 1.75 (m, 2H), 1.62 (d, *J* = 9 Hz, 2H), 1.60–1.45 (m, 6H), 1.28 (m, 2H); MS (ESI) *m/z* 318 (M + H)<sup>+</sup>.

***N*-(5,7-Dihydroxyadamantan-2-yl)-2-[4-(5-trifluoromethylpyridin-2-yl)piperazin-1-yl]propionamide (22g).** A solution of 2-bromo-*N*-(5,7-dihydroxyadamantan-2-yl)propionamide (0.17 g, 0.55 mmol) and 1-(5-trifluoromethylpyridin-2-yl)piperazine (0.13 g, 0.55 mmol) in 1:1 MeOH/CH<sub>3</sub>CN (4 mL) was treated with DIPEA (0.19 mL, 1.1 mmol) and heated at 70 °C overnight. The solvents were removed under reduced pressure, and the residue was purified by flash column chromatography on silica gel, 5–10% MeOH in CH<sub>2</sub>Cl<sub>2</sub> to provide **22g** (0.25 g, 96%). <sup>1</sup>H NMR (300 MHz, DMSO-*d*<sub>6</sub>)  $\delta$  8.40 (s, 1H), 7.79 (dd, *J* = 3, 8 Hz, 1H), 7.79 (dd, *J* = 3, 8 Hz, 1H), 7.62 (d, *J* = 8 Hz, 1H), 6.97 (d, *J* = 9 Hz, 1H), 4.54 (s, 1H), 4.50 (s, 1H), 3.62 (m, 4H), 3.30–3.05 (m, 4H), 2.55 (m, 2H), 2.01 (m, 2H), 1.80–1.40 (m, 4H), 1.40–1.20 (m, 6H), 1.10 (d, *J* = 8 Hz, 3H); MS (ESI) *m/z* 469 (M + H)<sup>+</sup>. Anal. (C<sub>23</sub>H<sub>31</sub>F<sub>3</sub>N<sub>4</sub>O<sub>3</sub>·0.4H<sub>2</sub>O) C, H, N.

***N*-(*E*)-5-Hydroxy-2-adamantyl]-2-methyl-2-[4-[5-(trifluoromethyl)pyridin-2-yl]piperazin-1-yl]propanamide (23).** A solution of **19** (160 mg, 0.50 mmol) in CH<sub>2</sub>Cl<sub>2</sub> (5 mL) and DIPEA (0.5 mL) was treated with HOBt (84 mg, 0.55 mmol), **5b** (100 mg, 0.60 mmol), and, 15 min later, EDCI (110 mg, 0.66 mmol). The reaction mixture was stirred at room temperature overnight and concentrated under reduced pressure. The residue was partitioned between water and EtOAc. The aqueous layer was extracted twice with EtOAc. The combined organic extracts were washed with saturated sodium bicarbonate solution and water, dried (MgSO<sub>4</sub>), and filtered. The filtrate was concentrated under reduced pressure and purified by reversed-phase HPLC to provide **23** as a white solid (160 mg, 69%). <sup>1</sup>H NMR (300 MHz, CDCl<sub>3</sub>)  $\delta$  8.41 (s, 1H), 7.67 (m, 2H), 6.66 (d, *J* = 9.1 Hz, 1H), 4.0 (d, *J* = 7.8 Hz, 1H), 3.66 (m, 4H), 2.64 (m, 4H), 2.23–2.1 (m, 3H), 1.9–1.63 (m, 10H), 1.25 (s, 6H); MS (APCI) *m/z* 467 (M + H)<sup>+</sup>. Anal. (C<sub>24</sub>H<sub>33</sub>F<sub>3</sub>N<sub>4</sub>O<sub>2</sub>·0.55H<sub>2</sub>O) C, H, N.

***N*-(3-Methylene-7-oxo-bicyclo[3.3.1]non-9-yl)-2-[4-(5-trifluoromethyl-pyridin-2-yl)-piperazin-1-yl]-isobutyramide (24).** A solution of **19** (130 mg, 0.41 mmol) in CH<sub>2</sub>Cl<sub>2</sub> (2 mL) and DMF

(0.5 mL) was treated with HOBt (67 mg, 0.44 mmol), **17** (69 mg, 0.42 mmol), and, 15 min later, EDCI (92 mg, 0.48 mmol). The reaction mixture was stirred at room temperature overnight and concentrated under reduced pressure. The residue was partitioned between water and EtOAc. The aqueous layer was extracted twice with EtOAc. The combined organic extracts were washed with saturated sodium bicarbonate solution and water, dried (MgSO<sub>4</sub>), and filtered. The filtrate was concentrated under reduced pressure, and the crude product was purified by flash column chromatography on silica gel with 10–40% acetone in hexane to provide **24** as a white solid (120 mg, 65%). <sup>1</sup>H NMR (400 MHz, CDCl<sub>3</sub>)  $\delta$  8.40 (s, 1H), 7.76 (s, 1H), 7.65 (dd, *J* = 9.05, 2.61 Hz, 1H), 6.63 (d, *J* = 9.21 Hz, 1H), 4.86 (s, 2H), 4.17 (d, *J* = 7.36 Hz, 1H), 3.60 (s, 4H), 2.60–2.67 (m, 4H), 2.52 (s, 4H), 2.30–2.40 (m, 6H), 1.27 (s, 6H); MS (ESI) *m/z* 465 (M + H)<sup>+</sup>.

***N*-(5,7-Dihydroxyadamantan-2-yl)-2-[4-(5-trifluoromethyl-pyridin-2-yl)-piperazin-1-yl]-isobutyramide (25).** A solution of **24** (30 mg, 0.065 mmol) in MeOH was treated with a catalytic amount of 48% aqueous hydrobromic acid and stirred at reflux overnight. The reaction mixture was concentrated under reduced pressure, and the residue was purified by reversed-phase HPLC to provide **25** as a white solid (10 mg, 35%). <sup>1</sup>H NMR (500 MHz, CDCl<sub>3</sub>)  $\delta$  8.40 (s, 1H), 7.59–7.66 (m, 2H), 6.65 (d, *J* = 8.73 Hz, 1H), 3.87 (d, *J* = 7.80 Hz, 1H), 3.65 (s, 4H), 2.63 (t, *J* = 4.99 Hz, 4H), 2.61 (s, 1H), 2.26 (d, *J* = 2.18 Hz, 2H), 1.84 (d, *J* = 11.85 Hz, 2H), 1.77 (s, 2H), 1.69 (dd, *J* = 12.32, 10.45 Hz, 4H), 1.58 (d, *J* = 5.61 Hz, 2H), 1.24 (s, 6H); MS (ESI) *m/z* 483 (M + H)<sup>+</sup>. HRMS (ESI; M<sup>+</sup>): calcd for C<sub>24</sub>H<sub>33</sub>F<sub>3</sub>N<sub>4</sub>O<sub>3</sub>, 483.25775; found, 483.25712. Analytical HPLC using a Phenomenex Luna analytical column and 10% CH<sub>3</sub>CN/0.1% TFA buffer (alternatively 0.01% ammonium acetate buffer) to 100% CH<sub>3</sub>CN gradient showed >95% purity.

***N*-(7-Hydroxy-5-methoxyadamantan-2-yl)-2-[4-(5-trifluoromethyl-pyridin-2-yl)-piperazin-1-yl]-isobutyramide (26).** A solution of **24** (30 mg, 0.065 mmol) in MeOH (0.5 mL) was treated with a catalytic amount of hydrobromic acid and stirred at reflux overnight. The reaction mixture was concentrated under reduced pressure, and the residue was purified by reversed-phase HPLC to provide **26** as a white solid (11 mg, 37%). <sup>1</sup>H NMR (500 MHz, CDCl<sub>3</sub>)  $\delta$  8.40 (s, 1H), 7.59–7.66 (m, 2H), 6.65 (d, *J* = 9.04 Hz, 1H), 3.86 (d, *J* = 8.11 Hz, 1H), 3.65 (s, 4H), 3.25 (s, 3H), 2.60–2.66 (m, 4H), 2.28 (d, *J* = 1.56 Hz, 2H), 1.84 (d, *J* = 11.85 Hz, 2H), 1.77 (s, 2H), 1.66–1.75 (m, 4H), 1.59 (s, 2H), 1.24 (s, 6H); MS (ESI) *m/z* 497 (M + H)<sup>+</sup>. HRMS (ESI; M<sup>+</sup>): calcd for C<sub>25</sub>H<sub>35</sub>F<sub>3</sub>N<sub>4</sub>O<sub>3</sub>, 497.27340; found, 497.27273. Analytical HPLC using a Phenomenex Luna analytical column and 10% CH<sub>3</sub>CN/0.1% TFA buffer (alternatively 0.01% ammonium acetate buffer) to 100% CH<sub>3</sub>CN gradient showed >95% purity.

***N*-(*E*)-5-Fluoro-2-adamantyl]-2-[4-[5-(trifluoromethyl)pyridin-2-yl]piperazin-1-yl]acetamide (27a).** A –78 °C solution of **22d** (66 mg, 0.15 mmol) in CH<sub>2</sub>Cl<sub>2</sub> (0.5 mL) was treated with DAST (0.020 mL, 0.16 mmol) and slowly warmed to room temperature over 6 h. The reaction mixture was quenched with saturated sodium bicarbonate solution (0.1 mL), filtered through a Celite cartridge, and purified by flash column chromatography on silica gel with 10–40% acetone in hexane to provide **27a** as a white solid (42 mg, 63%). <sup>1</sup>H NMR (300 MHz, CDCl<sub>3</sub>)  $\delta$  8.42 (s, 1H), 7.63 (m, 2H), 6.68 (d, *J* = 9.2 Hz, 1H), 4.09 (d, *J* = 8.5 Hz, 1H), 3.69 (s, 4H), 3.09 (s, 2H), 2.69 (s, 4H), 2.27–2.22 (m, 3H), 2.06 (m, 2H), 1.94 (m, 4H), 1.58–1.54 (m, 4H); (APCI) *m/z* 441 (M + H)<sup>+</sup>. Anal. (C<sub>22</sub>H<sub>28</sub>F<sub>4</sub>N<sub>4</sub>O·0.5C<sub>3</sub>H<sub>6</sub>O) C, H, N.

***N*-(*Z*)-5-Fluoro-2-adamantyl]-2-[4-[5-(trifluoromethyl)pyridin-2-yl]piperazin-1-yl]acetamide (27b).** Purification of the concentrated filtrate from the previous step by flash column chromatography on silica gel with 10–40% acetone in hexane provided **27b** (20 mg, 30%). <sup>1</sup>H NMR (300 MHz, CDCl<sub>3</sub>)  $\delta$  8.42 (s, 1H), 7.66 (m, 2H), 6.67 (d, *J* = 9.16 Hz, 1H), 3.95 (d, *J* = 5.09 Hz, 1H), 3.70 (s, 4H), 3.10 (s, 2H), 2.68 (s, 4H), 2.29 (m, 3H), 1.80–1.93 (m, 5H), 1.67–1.79 (m, 5H); (APCI) *m/z* 441 (M+H)<sup>+</sup>; HRMS (ESI; M<sup>+</sup>): calcd for C<sub>22</sub>H<sub>28</sub>F<sub>4</sub>N<sub>4</sub>O, 441.2199; found, 441.2271. Analytical HPLC using a Phenomenex Luna analytical column and

10% CH<sub>3</sub>CN/0.1%TFA buffer (alternatively 0.01% ammonium acetate buffer) to 100% CH<sub>3</sub>CN gradient showed >95% purity. Anal. (C<sub>22</sub>H<sub>28</sub>F<sub>4</sub>N<sub>4</sub>O·0.5C<sub>3</sub>H<sub>6</sub>O) C, H, N.

***E-N-(5-Methoxy-adamantan-2-yl)-2-[4-(5-trifluoromethyl-pyridin-2-yl)-piperazin-1-yl]-propionamide (27c)***. A solution of *N*-[(*E*)-5-hydroxy-2-adamantyl]-2-[4-[5-(trifluoromethyl)pyridin-2-yl]piperazin-1-yl]propanamide (**22f**; 35 mg, 0.077 mmol) in toluene (3 mL) was treated with sodium hydride (5.0 mg, 0.12 mmol) and methyl iodide (14 mg, 0.095 mmol). The reaction mixture was irradiated with microwaves at 160 °C for 8 h and concentrated under reduced pressure. The residue was purified by reversed-phase HPLC to provide **27c** (7.9 mg, 21%). <sup>1</sup>H NMR (500 MHz, DMSO-*d*<sub>6</sub>) δ 8.48 (s, 1H), 8.45 (d, 1H), 7.91 (dd, 1H), 7.07 (d, 1H), 4.05 (m, 1H), 3.83–3.90 (m, 1H), 3.45–3.35 (m, 4H), 3.11 (s, 3H), 2.07–2.04 (m, 4H), 1.86 (t, 3H), 1.65–1.79 (m, 7H), 1.47 (d, 3H), 1.40 (d, 3H); MS (ESI) *m/z* 467 (M + H)<sup>+</sup>. HRMS (ESI; M<sup>+</sup>): calcd for C<sub>24</sub>H<sub>34</sub>F<sub>3</sub>N<sub>4</sub>O<sub>2</sub>, 467.2628; found, 467.2630. Analytical HPLC using a Phenomenex Luna analytical column and 10% CH<sub>3</sub>CN/0.1%TFA buffer (alternatively 0.01% ammonium acetate buffer) to 100% CH<sub>3</sub>CN gradient showed >95% purity.

***N-(5-Fluoro-7-hydroxyadamantan-2-yl)-2-[4-(5-trifluoromethylpyridin-2-yl)piperazin-1-yl]propionamide (27d)***. A –78 °C mixture of **22g** (0.10 g, 0.21 mmol) in CH<sub>2</sub>Cl<sub>2</sub> (5 mL) was treated with DAST (0.056 mL, 0.43 mmol) and stirred, warming to room temperature overnight. The reaction mixture was quenched with saturated sodium bicarbonate solution (3 mL) and extracted with 10% MeOH in CH<sub>2</sub>Cl<sub>2</sub> (3 ×). The combined organic extracts were dried (Na<sub>2</sub>SO<sub>4</sub>), filtered, and concentrated under reduced pressure. The residue was purified by flash column chromatography (silica gel, 5% MeOH in CH<sub>2</sub>Cl<sub>2</sub>) to provide **27d** (5 mg, 5%). <sup>1</sup>H NMR (500 MHz, CDCl<sub>3</sub>) δ 8.41 (s, 1H), 7.65 (dd, *J* = 3, 8 Hz, 1H), 7.58 (d, *J* = 7 Hz, 1H), 6.66 (d, *J* = 9 Hz, 1H), 3.90 (m, 1H), 3.68 (m, 4H), 3.15 (q, *J* = 7 Hz, 1H), 2.70 (m, 2H), 2.62 (m, 2H), 2.35 (s, 2H), 1.96 (m, 2H), 1.90–1.65 (m, 6H), 1.61 (m, 2H), 1.27 (d, *J* = 8 Hz, 3H); MS (ESI) *m/z* 471 (M + H)<sup>+</sup>; HRMS (ESI; M<sup>+</sup>): calcd for C<sub>23</sub>H<sub>30</sub>F<sub>4</sub>N<sub>4</sub>O<sub>2</sub>, 471.23777; found, 471.2375. Analytical HPLC using a Phenomenex Luna analytical column and 10% CH<sub>3</sub>CN/0.1%TFA buffer (alternatively 0.01% ammonium acetate buffer) to 100% CH<sub>3</sub>CN gradient showed >95% purity.

***N-(5-Fluoro-7-hydroxyadamantan-2-yl)-2-[4-(5-trifluoromethylpyridin-2-yl)piperazin-1-yl]propionamide (27e)***. Purification of the concentrated filtrate from the previous step by flash column chromatography (silica gel, 5% MeOH in CH<sub>2</sub>Cl<sub>2</sub>) provided **27e** (5 mg, 5%). <sup>1</sup>H NMR (500 MHz, CDCl<sub>3</sub>) δ 8.41 (s, 1H), 7.64 (dd, *J* = 3, 8 Hz, 1H), 7.57 (d, *J* = 7 Hz, 1H), 6.65 (d, *J* = 9 Hz, 1H), 3.92 (m, 1H), 3.67 (m, 4H), 3.13 (q, *J* = 7 Hz, 1H), 2.69 (m, 2H), 2.60 (m, 2H), 2.35 (m, 2H), 2.02 (m, 2H), 1.95 (d, *J* = 3 Hz, 2H), 1.90–1.65 (m, 4H), 1.61 (m, 2H), 1.26 (d, *J* = 8 Hz, 3H); MS (ESI) *m/z* 471 (M + H)<sup>+</sup>; HRMS (ESI; M<sup>+</sup>): calcd for C<sub>23</sub>H<sub>30</sub>F<sub>4</sub>N<sub>4</sub>O<sub>2</sub>, 471.23777; found, 471.23675. Analytical HPLC using a Phenomenex Luna analytical column and 10% CH<sub>3</sub>CN/0.1%TFA buffer (alternatively 0.01% ammonium acetate buffer) to 100% CH<sub>3</sub>CN gradient showed >95% purity.

***N-(5-Hydroxy-adamantan-2-yl)-2-(3-trifluoromethyl-pyrrolidin-1-yl)-acetamide (28)***. A solution of 2-chloro-*N*-(2-hydroxyadamantan-1-yl)-acetamide (23 mg, 0.10 mmol) in MeOH (0.5 mL) and DIPEA (21 μL, 0.12 mmol) was treated with 3-*S*-trifluoromethyl pyrrolidine (17 mg, 0.12 mmol) and stirred at 70 °C overnight. The MeOH was removed under reduced pressure. The residue was dissolved in CH<sub>2</sub>Cl<sub>2</sub>, washed twice with water, dried (MgSO<sub>4</sub>), and filtered. The filtrate was concentrated under reduced pressure and purified by reversed-phase HPLC to provide **28** as a white solid (24 mg, 70%). <sup>1</sup>H NMR (500 MHz, pyridine-*d*<sub>5</sub>) 7.73 (s, 1H), 5.87 (s, 1H), 4.35 (s, 1H), 3.75 (d, *J* = 16.85 Hz, 1H), 3.61 (d, *J* = 17.47 Hz, 1H), 3.55 (d, *J* = 16.85 Hz, 1H), 3.14–3.18 (m, 1H), 2.61 (td, *J* = 9.36, 6.24 Hz, 1H), 2.25 (s, 2H), 2.10 (s, 3H), 1.96–2.05 (m, 5H), 1.84–1.93 (m, 3H), 1.78 (s, 1H), 1.70 (s, 1H), 1.52 (t, *J* = 9.83 Hz, 2H); MS (ESI) *m/z* 347 (M + H)<sup>+</sup>. HRMS (ESI; M<sup>+</sup>): calcd for C<sub>17</sub>H<sub>25</sub>F<sub>3</sub>N<sub>2</sub>O<sub>2</sub>, 347.19404; found, 347.19367. Analytical HPLC using a Phenomenex Luna analytical column and

10% CH<sub>3</sub>CN/0.1%TFA buffer (alternatively 0.01% ammonium acetate buffer) to 100% CH<sub>3</sub>CN gradient showed >95% purity.

***E-(2R)-(3R-Fluoro-pyrrolidin-1-yl)-N-(5-hydroxy-adamantan-2-yl)-propionamide (29)***. A solution of (*S*)-2-bromo-propionic acid (1.5 g, 10 mmol) in CH<sub>2</sub>Cl<sub>2</sub> (100 mL) was treated with HOBT (1.7 g, 11 mmol), **5b** (1.7 g, 10 mmol), and, 15 min later, with EDCI (2.4 g, 12 mmol). The reaction mixture was stirred at room temperature overnight and concentrated under reduced pressure. The residue was partitioned between water and EtOAc. The aqueous layer was extracted twice with EtOAc. The combined organic extracts were washed with saturated sodium bicarbonate solution and water, dried (MgSO<sub>4</sub>), and filtered. The filtrate was concentrated under reduced pressure and purified by flash column chromatography on silica gel with 10–40% acetone in hexane to provide *E*-(*S*)-2-bromo-*N*-(5-hydroxy-adamantan-2-yl)-propionamide as a white solid (2.5 g, 83%).

A solution of the propionamide (100 mg, 0.33 mmol) and hydrochloride of (*R*)-3-fluoropyrrolidine (41 mg, 0.33 mmol) in CH<sub>2</sub>Cl<sub>2</sub> (1 mL) and triethylamine (0.1 mL) was stirred at 50 °C overnight. The solvent was removed under reduced pressure, and the residue was purified by reversed-phase HPLC to provide **29** as a white solid (62 mg, 61%). <sup>1</sup>H NMR (300 MHz, CDCl<sub>3</sub>) 7.42 (s, 1H), 5.12–5.23 (d, *J* = 55 Hz, 1H), 4.01 (d, *J* = 8.5 Hz, 1H), 2.93–3.16 (m, 3H), 2.20–2.50 (m, 2H), 2.23–2.1 (m, 5H), 1.9–1.88 (m, 2H), 1.7–1.8 (m, 6H), 1.5–1.53 (m, 2H), 1.33 (d, *J* = 5.2 Hz, 3H); MS (APCI<sup>+</sup>) *m/z* 311 (M + H)<sup>+</sup>. HRMS (ESI; M<sup>+</sup>): calcd for C<sub>17</sub>H<sub>27</sub>FN<sub>2</sub>O<sub>2</sub>, 311.21293; found, 311.21215. Analytical HPLC using a Phenomenex Luna analytical column and 10% CH<sub>3</sub>CN/0.1%TFA buffer (alternatively 0.01% ammonium acetate buffer) to 100% CH<sub>3</sub>CN gradient showed >95% purity.

***E-(2S)-(3R-Fluoro-pyrrolidin-1-yl)-N-(5-hydroxy-adamantan-2-yl)-propionamide (30)***. A solution of (*R*)-2-bromo-propionic acid (1.5 g, 10 mmol) in CH<sub>2</sub>Cl<sub>2</sub> (100 mL) was treated with HOBT (1.7 g, 11 mmol), **5b** (1.7 g, 10 mmol), and, 15 min later, with EDCI (2.4 g, 12 mmol). The reaction mixture was stirred at room temperature overnight and concentrated under reduced pressure. The residue was partitioned between water and EtOAc. The aqueous layer was extracted twice with EtOAc. The combined organic extracts were washed with saturated sodium bicarbonate solution and water, dried (MgSO<sub>4</sub>), and filtered. The filtrate was concentrated under reduced pressure and purified by flash column chromatography on silica gel with 10–40% acetone in hexane to provide *E*-(*R*)-2-bromo-*N*-(5-hydroxy-adamantan-2-yl)-propionamide as a white solid (2.4 g, 81%).

A solution of the propionamide (100 mg, 0.33 mmol) and hydrochloride of (*R*)-3-fluoropyrrolidine (41 mg, 0.33 mmol) in CH<sub>2</sub>Cl<sub>2</sub> (1 mL) and triethylamine (0.1 mL) was stirred at 50 °C overnight. The solvent was removed under reduced pressure, and the residue was purified by reversed-phase HPLC to provide **30** as a white solid (60 mg, 59%). <sup>1</sup>H NMR (500 MHz, CDCl<sub>3</sub>) 7.48 (s, 1H), 5.12–5.23 (d, *J* = 55 Hz, 1H), 4.01 (d, *J* = 8.24 Hz, 1H), 3.11 (s, 1H), 3.00 (s, 2H), 2.50 (d, *J* = 10.68 Hz, 1H), 2.16 (s, 2H), 2.11 (s, 3H), 1.90 (d, *J* = 11.60 Hz, 2H), 1.77 (d, *J* = 1.53 Hz, 4H), 1.75 (d, *J* = 2.75 Hz, 2H), 1.71 (s, 2H), 1.43 (s, 1H), 1.28–1.36 (m, 3H); MS (APCI) *m/z* 311 (M + H)<sup>+</sup>. HRMS (ESI; M<sup>+</sup>): calcd for C<sub>17</sub>H<sub>27</sub>FN<sub>2</sub>O<sub>2</sub>, 311.21293; found, 311.21213. Analytical HPLC using a Phenomenex Luna analytical column and 10% CH<sub>3</sub>CN/0.1%TFA buffer (alternatively 0.01% ammonium acetate buffer) to 100% CH<sub>3</sub>CN gradient showed >95% purity.

***E-2-Bromo-N-(2-hydroxy-adamantan-1-yl)-propionamide***. A 0 °C solution of 1-amino-adamantan-2-ol (**5b**; 0.43 g, 2.6 mmol) in CH<sub>2</sub>Cl<sub>2</sub> (10 mL) and DIPEA (0.54 mL, 3.1 mmol) was treated with 2-bromopropionyl chloride (0.26 mL, 2.6 mmol). The reaction mixture was stirred at room temperature for 2 h and concentrated under reduced pressure. The residue was purified by flash column chromatography on silica gel with 4:1 hexane/acetone to provide the *E*-2-bromo-*N*-(2-hydroxy-adamantan-1-yl)-propionamide as a beige solid (0.39 g, 50%).

***2-[3-(2-Fluoro-phenoxy)-azetid-1-yl]-N-(5-hydroxy-adamantan-2-yl)-propionamide (31)***. A solution of *E*-2-bromo-*N*-(5-hydroxy-adamantan-2-yl)-propionamide (30 mg, 0.10 mmol) in

MeOH (0.5 mL) and DIPEA (21  $\mu$ L, 0.12 mmol) was treated with 3-(2-fluoro-phenoxy)-azetidone (20 mg, 0.12 mmol) and stirred at 70 °C overnight. The MeOH was removed under reduced pressure. The residue was dissolved in CH<sub>2</sub>Cl<sub>2</sub>, washed twice with water, dried (MgSO<sub>4</sub>), and filtered. The filtrate was concentrated under reduced pressure and purified by reversed-phase HPLC to provide **31** as a white solid (27 mg, 70%). <sup>1</sup>H NMR (500 MHz, pyridine-*d*<sub>5</sub>) 7.40 (d, *J* = 7.80 Hz, 1H), 7.23–7.26 (m, 1H), 7.09 (tt, *J* = 7.80, 1.25 Hz, 1H), 6.94–6.98 (m, 2H), 4.92 (m, 1H), 4.27 (d, *J* = 7.49 Hz, 1H), 3.95 (s, 1H), 3.79 (s, 1H), 3.39 (dd, *J* = 7.80, 5.30 Hz, 1H), 3.34 (dd, *J* = 7.49, 5.61 Hz, 1H), 3.18 (d, *J* = 6.86 Hz, 1H), 2.19–2.26 (m, 2H), 2.09 (d, *J* = 10.60 Hz, 2H), 2.03 (s, 1H), 1.95–1.99 (m, 4H), 1.84 (d, *J* = 13.10 Hz, 2H), 1.47 (d, *J* = 12.16 Hz, 2H), 1.29 (d, *J* = 6.86 Hz, 3H); MS (ESI) *m/z* 389 (M + H)<sup>+</sup>. Anal. (C<sub>22</sub>H<sub>29</sub>N<sub>2</sub>O<sub>3</sub>·0.3CF<sub>3</sub>CO<sub>2</sub>H) C, H, N.

***N*-[(1*R*,3*S*)-5-Hydroxy-2-adamantyl]-2-(6,7,9,10-tetrahydro-8*H*-[1,3]dioxolo[4,5-*g*] [3]benzazepin-8-yl)propanamide (32). (4-Hydroxymethyl-benzo[1,3]dioxol-5-yl)methanol.** A 0 °C solution of 1.0 M borane–THF complex (200 mL, 200 mmol) was treated portionwise with 5-formyl-benzo[1,3]dioxole-4-carboxylic acid (10 g, 51 mmol).<sup>45</sup> Upon the completion of the addition, the reaction mixture was stirred at room temperature for 1 h. The reaction mixture was cooled to 0 °C, quenched with water, and concentrated under reduced pressure. The residue was acidified with 3 N hydrochloric acid solution and extracted with chloroform. The combined organic extracts were dried (Na<sub>2</sub>SO<sub>4</sub>), filtered, and concentrated under reduced pressure to afford the alcohol (8.5 g, 92%). MS (DCI) *m/z* 182 (M + H)<sup>+</sup>.

**4,5-Bis-chloromethyl-benzo[1,3]dioxole.** A 0 °C solution of (4-hydroxymethyl-benzo[1,3]dioxol-5-yl)methanol (8.5 g, 47.0 mmol) from the previous step in CH<sub>2</sub>Cl<sub>2</sub> (50 mL) was treated with thionyl chloride (17 mL, 230 mmol). The reaction mixture was stirred at room temperature for 1 h and concentrated under reduced pressure to afford the title compound (10 g, 100%). MS (DCI) *m/z* 218 (M + H)<sup>+</sup>.

**(4-Cyanomethyl-benzo[1,3]dioxol-5-yl)acetonitrile.** A 0 °C suspension of sodium cyanide (7.4 g, 150 mmol) in dimethyl sulfoxide (80 mL) was treated portionwise with 4,5-bis-chloromethyl-benzo[1,3]dioxole (10 g, 47.0 mmol) from the previous step. The reaction mixture was stirred at room temperature for 2 h. Ice was added to the reaction mixture, and the solids that formed were filtered off and washed with water. The solids were dissolved in chloroform, and the solution was washed with 1 N sodium hydroxide solution, dried (Na<sub>2</sub>SO<sub>4</sub>), filtered, and concentrated under reduced pressure. The residue was purified by flash column chromatography on a silica gel column with 30% EtOAc in hexane to provide the title compound (6.0 g, 64%). MS (DCI) *m/z* 201 (M + H)<sup>+</sup>.

**7,8,9,10-Tetrahydro-6*H*-1,3-dioxo-8-azacyclohepta[*e*]indene.** (4-Cyanomethyl-benzo[1,3]dioxol-5-yl)acetonitrile (6.0 g, 30 mmol) from the previous step was reductively cyclized with Raney–nickel (1.2 g) under high pressure (1100 psi) in a 10% ammonia in ethanol solution (120 mL) at 100 °C for 1 h. The reaction mixture was cooled, and the catalyst was filtered off and washed with hot EtOH. The filtrate was concentrated under reduced pressure, and the residue was purified by flash column chromatography on a silica gel column with 30% MeOH in CH<sub>2</sub>Cl<sub>2</sub> to provide the title compound (23 mg, 0.4%). MS (DCI) *m/z* 192 (M + H)<sup>+</sup>.

***N*-[(1*R*,3*S*)-5-Hydroxy-2-adamantyl]-2-(6,7,9,10-tetrahydro-8*H*-[1,3]dioxolo[4,5-*g*] [3]benzazepin-8-yl)propanamide (32).** A solution of *E*-2-bromo-*N*-(5-hydroxy-adamantan-2-yl)propanamide (30 mg, 0.10 mmol) in MeOH (0.5 mL) and DIPEA (21  $\mu$ L, 0.12 mmol) was treated with 7,8,9,10-tetrahydro-6*H*-1,3-dioxo-8-azacyclohepta[*e*]indene from the previous step (23 mg, 0.12 mmol) and stirred at 70 °C overnight. The MeOH was removed under reduced pressure. The residue was dissolved in CH<sub>2</sub>Cl<sub>2</sub>, washed twice with water, dried (MgSO<sub>4</sub>), and filtered. The filtrate was concentrated under reduced pressure and purified by reversed-phase HPLC to provide **31** as a white solid (28 mg, 69%). <sup>1</sup>H NMR (400 MHz, DMSO-*d*<sub>6</sub>) 7.75 (d, *J* = 8 Hz, 1H), 6.60 (m, 2H), 5.93

(s, 2H), 3.77 (m, 1H), 3.39 (q, *J* = 6.76 Hz, 1H), 2.80 (m, 4H), 2.65–2.50 (m, 4H), 2.05–1.90 (m, 3H), 1.80–1.55 (m, 8H), 1.40 (m, 2H), 1.03 (d, *J* = 6.86 Hz, 3H); MS (ESI) *m/z* 413 (M + H)<sup>+</sup>. Anal. (C<sub>24</sub>H<sub>32</sub>N<sub>2</sub>O<sub>4</sub>·0.1CF<sub>3</sub>CO<sub>2</sub>H) C, H, N.

**Assay Protocols. Materials.** [1,2(*n*)-<sup>3</sup>H-cortisone, [1,2,6,7-(<sup>3</sup>H)]-hydrocortisone, and SPA beads were purchased from GE Healthcare. NADPH, NAD<sup>+</sup>, 18 $\beta$ -glycyrrhetic acid (18 $\beta$ -GA), and cortisone were obtained from Sigma-Aldrich. Glucose-6-phosphate (G-6-P) and glucose-6-dehydrogenase (G-6-PDH) were procured from Roche Diagnostics. Anti-cortisol monoclonal antibody and fluorescein-labeled cortisol were obtained from Abbott Laboratory's Diagnostic Division. Dulbecco's Modified Eagle Medium (DMEM), Dulbecco's Phosphate Buffered Saline (PBS), fetal bovine serum (FBS), geneticin, and antibiotic–antimycotic were purchased from Invitrogen Corp/GIBCO.

**Human and Mouse HSD1 SPA Assays.** The *in vitro* 11 $\beta$ -HSD1 enzymatic assays are similar to the methods previously described.<sup>28a</sup> Truncated human or mouse 11 $\beta$ -HSD1, lacking the first 24 amino acids, was expressed in *E. coli* using the pET28 expression system, and the crude lysates were used as the enzyme source. The reaction was carried out with a total substrate (cortisone) concentration of 175 nM, which contained 75 nM <sup>3</sup>H-cortisone and 181  $\mu$ M of the cofactor NADPH in 50 mM Tris-HCl, at pH 7.2 with 1 mM EDTA. The final enzyme concentration was 0.015 mg/mL to keep the substrate consumption rate below 25% at the end of the reaction. To ensure the reaction proceeds in the reductase direction, a NADPH regeneration system with 1 mM G-6-P and 1 unit/mL of G-6-PDH was included in the reaction. After incubating at room temperature for 30 min, the reaction was terminated by adding the nonselective 11 $\beta$ -HSD1 inhibitor 18 $\beta$ -GA. The radioactive cortisol generated in the assay was captured by a monoclonal anti-cortisol antibody and SPA beads coated with anti-mouse antibodies. The plate was read using a Microbeta Liquid Scintillation Counter (Perkin-Elmer Life Sciences). The percent inhibition was calculated relative to a noninhibited control and plotted against compound concentration to generate the IC<sub>50</sub> results.

**Human and Mouse HSD2 SPA Assays.** The *in vitro* 11 $\beta$ -HSD2 dehydrogenase assays were developed using the cell lysates that had the full length human or mouse 11 $\beta$ -HSD2 cDNA overexpressed using the baculovirus expression system. The reaction was carried out with 6 nM of <sup>3</sup>H-cortisol and 250  $\mu$ M of the cofactor NAD<sup>+</sup> in the 50 mM Tris-HCl/1 mM EDTA buffer containing 1 mM magnesium chloride, at pH 7.2. The final enzyme concentration was 0.2 mg/mL per well. After incubating at room temperature for 30 min, the reaction was terminated by adding 18 $\beta$ -GA. The radioactive cortisol remaining in the well was captured by a monoclonal anticortisol antibody and SPA beads coated with anti-mouse antibodies. The percent inhibition was calculated relative to an uninhibited control and plotted against compound concentration to generate the IC<sub>50</sub> results.

**HEK HSD1 Cellular FPIA Assay.** Cellular activity of the compounds was evaluated in HEK293 cells, which were stably transfected with full length human 11 $\beta$ -HSD1 cDNA. Cells were plated on poly-D-lysine coated plates (Becton Dickinson Biocoat 35-4461) in DMEM media containing 10% FBS, 300  $\mu$ g/mL geneticin, 100 units/mL penicillin, 100  $\mu$ g/mL streptomycin, and 0.25  $\mu$ g/mL fungizone. The cells were pretreated with compounds for 30 min, followed by incubation with 1  $\mu$ M of substrate (cortisone) in PBS buffer for 2 h at 37 °C in a 5% CO<sub>2</sub> atmosphere. The cell media were harvested, and the cortisol concentration in the media was determined by fluorescence polarization immunoassay (FPIA). A mixture of fluorescein-labeled cortisol and monoclonal anti-cortisol antibody were added to the well in the FPIA diluent buffer (Abbott Laboratories) to a final concentration 4 nM (cortisol) and 10 nM (mAb). The resulting fluorescent signal was read using an Analyst plate reader (LJL). The percent inhibition was calculated relative to an uninhibited control and plotted against compound concentration to generate the IC<sub>50</sub> results.

**Metabolic Stability Assay. Metabolic Incubation.** Each compound (1  $\mu$ M) was incubated, in duplicate, with pooled microsomal protein (0.2 – 0.5 mg/mL) in 50 mM potassium phosphate buffer

(pH 7.4) in a final incubation volume of 3 mL. Following a 5 min preincubation period at 37 °C, the reaction was initiated by adding NADPH (1 mM). Aliquots (200  $\mu$ L) were transferred to new tubes containing 100  $\mu$ L of acetonitrile and methanol (50:50, v/v) at 0, 5, 10, 15, 20, and 30 min after initiation. These samples were vortexed and centrifuged (16 000 rpm, 10 min), and the supernatant was analyzed by HPLC-tandem mass spectrometry (HPLC-MS/MS) as described below. The compound remaining in the incubation mixture was measured, and the *in vitro* half-life of substrate depletion was determined and converted into its hepatic intrinsic clearance value.<sup>46</sup>

**HPLC/MS Analysis.** Concentrations of each compound were determined by HPLC-MS/MS. The HPLC/MS system consisted of an Agilent 1100 series solvent delivery system and an automatic injector (Agilent Technologies, Waldbronn, Germany) and an API 2000 mass spectrometer with a turbo ionspray interface (MDS SCIEX, Ontario, Canada). A Luna C8(2) column (50  $\times$  2.0 mm, particle size 3  $\mu$ M, Phenomenex, Torrance, CA) was used for all compounds at room temperature. The mobile phase consisted of (A) 10 mM ammonium acetate (pH 3.3, adjusted with formic acid) and (B) 100% acetonitrile and delivered at a flow rate of 0.2 mL/minute. Elution was achieved by a linear gradient of 0–100% B over 3 min, then held 100% B for 4 min, and returned to 100% A in 1 min. The column was equilibrated for 7 min before the next injection.

**Ex Vivo HSD1 Assay.** Compounds were dissolved in 1% Tween 80 in 0.2% hydroxypropyl methylcellulose and administered to DIO mice as a single oral dose at 30 mg/kg. At 1, 7, and 16 h post-dose, fresh tissues including liver, adipose tissue (epididymal fat pad), and brain were removed, immersed in PBS buffer, and weighed. The total volume of PBS buffer added was equivalent to approximately five times the mass of tissue. Tissues were minced into 2–3 mm pieces, and the substrate (cortisone) was added to a final concentration of 10  $\mu$ M. The tissues were then incubated at 37 °C in a 5% CO<sub>2</sub> atmosphere for 20 min for liver and 3 h for brain and adipose tissue. The cortisol concentration in the media was determined by LC-MS detection.<sup>47</sup> The percent inhibition of 11 $\beta$ -HSD1 activity was calculated relative to a vehicle control treated group.

**Acknowledgment.** We thank Dr. Lan Gao and Mr. Steven P. Cepa for the LC/MS measurement of cortisol and Dr. Steven J. Richards and Dr. Andrew J. Souers for help in the preparation of this manuscript.

**Supporting Information Available:** X-ray crystallographic ORTEP structure and data for compound ( $\pm$ )-**22f** and elemental analyses. This material is available free of charge via the Internet at <http://pubs.acs.org>.

## References

- (1) (a) Trevisan, M.; Liu, J.; Bahsas, F. B.; Menotti, A. Syndrome X and mortality: A population-based study. Risk factor and life expectancy research group. *Am. J. Epidemiol.* **1998**, *148*, 958–966. (b) Isomaa, B.; Almgren, P.; Tuomi, T.; Forsen, B.; Lahti, K.; Nissen, M.; Taskinen, M. R.; Groop, L. Cardiovascular morbidity and mortality associated with the metabolic syndrome. *Diabetes Care* **2001**, *24*, 683–689. (c) Tomlinson, J. W.; Stewart, P. M. Mechanisms of disease: Selective inhibition of 11 $\beta$ -hydroxysteroid dehydrogenase type 1 as a novel treatment for the metabolic syndrome. *Nat. Clin. Pract. Endocrinol. Metab.* **2005**, *1*, 92–99. (d) Wang, M. The role of glucocorticoid action in the pathophysiology of the metabolic syndrome. *Nutr. Metab.* **2005**, *2*, 1–14.
- (2) Alberti, K. G. M. M.; Zimmet, P.; Shaw, J. Metabolic syndrome—a new world definition. A consensus statement from the international diabetes federation. *Diabetes Med.* **2006**, *23*, 469–480.
- (3) Arnaldi, G.; Angeli, A.; Atkinson, A. B.; Bertagna, X.; Cavagnini, F.; Chrousos, G. P.; Fava, G. A.; Findling, J. W.; Gaillard, R. C.; Grossman, A. B.; Kola, B.; Lacroix, A.; Mancini, T.; Mantero, F.; Newell-Price, J.; Nieman, L. K.; Sonino, N.; Vance, M. L.; Giustina, A.; Boscaro, M. Diagnosis and complications of Cushing's syndrome: A consensus statement. *J. Clin. Endocrinol. Metab.* **2003**, *88*, 5593–5602.
- (4) (a) Watanabe, K.; Adachi, A.; Nakamura, R. Reversible panhypopituitarism due to Cushing's syndrome. *Arch. Intern. Med.* **1988**, *148*, 1358–1360. (b) McEwen, B. S. Cortisol, Cushing's syndrome, and a shrinking brain—new evidence for reversibility. *J. Clin. Endocrinol. Metab.* **2002**, *87*, 1947–1948. (c) Inagaki, K.; Otsuka, F.; Miyoshi, T.; Watanabe, N.; Suzuki, J.; Ogura, T.; Makino, H. Reversible pituitary dysfunction in a patient with Cushing's syndrome discovered as adrenal incidentaloma. *Endocr. J.* **2004**, *51*, 201–206.
- (5) Fraser, R.; Ingram, M. C.; Anderson, N. H.; Morrison, C.; Davies, E.; Connell, J. M. C. Cortisol effects on body mass, blood pressure, and cholesterol in the general population. *Hypertension* **1999**, *33*, 1364–1368.
- (6) (a) Seckl, J. R.; Walker, B. R. Minireview: 11 $\beta$ -Hydroxysteroid dehydrogenase type 1—A tissue-specific amplifier of glucocorticoid action. *Endocrinology* **2001**, *142*, 1371–1376. (b) Tomlinson, J. W.; Walker, E. A.; Bujalska, I. J.; Draper, N.; Lavery, G. G.; Cooper, M. S.; Hewison, M.; Stewart, P. M. 11 $\beta$ -hydroxysteroid dehydrogenase type 1: A tissue-specific regulator of glucocorticoid response. *Endocr. Rev.* **2004**, *25*, 831–866. (c) Wake, D. J.; Walker, B. R. Inhibition of 11 $\beta$ -hydroxysteroid dehydrogenase type 1 in obesity. *Endocrine* **2006**, *29*, 101–108.
- (7) (a) Amelung, D.; Hubener, H. J.; Roka, L.; Meyerheim, G. Conversion of cortisone to compound F. *J. Clin. Endocrinol. Metab.* **1953**, *13*, 1125–1126. (b) Lakshmi, V.; Monder, C. Purification and characterization of the corticosteroid 11 $\beta$ -dehydrogenase component of the rat liver 11 $\beta$ -hydroxysteroid dehydrogenase complex. *Endocrinology* **1988**, *123*, 2390–2398. (c) Edwards, C. R. W.; Stewart, P. M.; Burt, D.; Brett, L.; McIntyre, M. A.; Sutanto, W. S.; De Kloet, E. R.; Monder, C. Localization of 11 $\beta$ -hydroxysteroid dehydrogenase—tissue specific protector of the mineralocorticoid receptor. *Lancet* **1988**, *2*, 986–989. (d) Funder, J. W.; Pearce, P. T.; Smith, R.; Smith, A. I. Mineralocorticoid action: Target tissue specificity is enzyme, not receptor, mediated. *Science* **1988**, *242*, 583–585.
- (8) (a) Agarwal, A. K.; Monder, C.; Eckstein, B.; White, P. C. Cloning and expression of rat cDNA encoding corticosteroid 11 $\beta$ -dehydrogenase. *J. Biol. Chem.* **1989**, *264*, 18939–18943. (b) Monder, C.; White, P. C. 11 $\beta$ -Hydroxysteroid dehydrogenase. *Vitam. Horm.* **1993**, *47*, 187–271. (c) Low, S. C.; Chapman, K. E.; Edwards, C. R. W.; Seckl, J. R. "Liver-type" 11 $\beta$ -hydroxysteroid dehydrogenase cDNA encodes reductase but not dehydrogenase activity in intact mammalian COS-7 cells. *J. Mol. Endocrinol.* **1994**, *13*, 167–174. (d) Bujalska, I. J.; Kumar, S.; Stewart, P. M. Does central obesity reflect "Cushing's disease of the omentum"? *Lancet* **1997**, *349*, 1210–1213. (e) Katz, J. R.; Mohamed-Ali, V.; Wood, P. J.; Yudkin, J. S.; Coppack, S. W. An in vivo study of the cortisol-cortisone shuttle in subcutaneous abdominal adipose tissue. *Clin. Endocrinol.* **1999**, *50*, 63–68. (f) Stewart, P. M.; Krozowski, Z. S. 11 $\beta$ -Hydroxysteroid dehydrogenase. *Vitam. Horm.* **1999**, *57*, 249–324. (g) Jamieson, P. M.; Walker, B. R.; Chapman, K. E.; Andrew, R.; Rossiter, S.; Seckl, J. R. 11 $\beta$ -Hydroxysteroid dehydrogenase type 1 is a predominant 11 $\beta$ -reductase in the intact perfused rat liver. *J. Endocrinol.* **2000**, *165*, 685–692.
- (9) (a) Brown, R. W.; Chapman, K. E.; Edwards, C. R. W.; Seckl, J. R. Human placental 11 $\beta$ -hydroxysteroid dehydrogenase: Evidence for and partial purification of a distinct NAD-dependent isoform. *Endocrinology* **1993**, *132*, 2614–2621. (b) Albiston, A. L.; Obeyesekere, V. R.; Smith, R. E.; Krozowski, Z. S. Cloning and tissue distribution of the human 11 $\beta$ -hydroxysteroid dehydrogenase type 2 enzyme. *Mol. Cell. Endocrinol.* **1994**, *105*, R11–R17. (c) Agarwal, A. K.; Mune, T.; Monder, C.; White, P. C. NAD<sup>+</sup>-dependent isoform of 11 $\beta$ -hydroxysteroid dehydrogenase. Cloning and characterization of cDNA from sheep kidney. *J. Biol. Chem.* **1994**, *269*, 25959–25962.
- (10) Arriza, J. L.; Weinberger, C.; Cerelli, G.; Glase, T. M.; Handelin, B. L.; Housman, D. E.; Evans, R. M. Cloning of human mineralocorticoid receptor complementary DNA: structural and functional kinship with the glucocorticoid receptor. *Science* **1987**, *237*, 268–275.
- (11) (a) Mune, T.; Rogerson, F. M.; Nikkila, H.; Agarwal, A. K.; White, P. C. Human hypertension caused by mutations in the kidney isoenzyme of 11 $\beta$ -hydroxysteroid dehydrogenase. *Nat. Genet.* **1995**, *10*, 394–399. (b) Dave-Sharma, S.; Wilson, R. C.; Harbison, M. D.; Newfield, R.; Azar, M. R.; Krozowski, Z. S.; Funder, J. W.; Shackleton, C. H. L.; Bradlow, H. L.; Wei, J.-Q.; Hertecant, J.; Moran, A.; Neiberger, R. E.; Balfe, J. W.; Fattah, A.; Daneman, D.; Akkurt, H. I.; De Santis, C.; New, M. I. Examination of genotype and phenotype relationships in 14 patients with apparent mineralocorticoid excess. *J. Clin. Endocrinol. Metab.* **1998**, *83*, 2244–2254.

- (12) Kotelevtsev, Y.; Holmes, M. C.; Burchell, A.; Houston, P. M.; Schmol, D.; Jamieson, P.; Best, R.; Brown, R.; Edwards, C. R. W.; Seckl, J. R.; Mullins, J. J. 11 $\beta$ -Hydroxysteroid dehydrogenase type 1 knockout mice show attenuated glucocorticoid-inducible responses and resist hyperglycemia on obesity or stress. *Proc. Natl. Acad. Sci. U.S.A.* **1997**, *94*, 14924–14929.
- (13) Morton, N. M.; Holmes, M. C.; Fievet, C.; Staels, B.; Tailleux, A.; Mullins, J. J.; Seckl, J. R. Improved lipid and lipoprotein profile, hepatic insulin sensitivity, and glucose tolerance in 11 $\beta$ -hydroxysteroid dehydrogenase type 1 null mice. *J. Biol. Chem.* **2001**, *276*, 41293–41300.
- (14) (a) Masuzaki, H.; Paterson, J.; Shinyama, H.; Morton, N. M.; Mullins, J. J.; Seckl, J. R.; Flier, J. S. A transgenic model of visceral obesity and the metabolic syndrome. *Science* **2001**, *294*, 2166–2170. (b) Masuzaki, H.; Yamamoto, H.; Kenyon, C. J.; Elmquist, J. K.; Morton, N. M.; Paterson, J. M.; Shinyama, H.; Sharp, M. G. F.; Fleming, S.; Mullins, J. J.; Seckl, J. R.; Flier, J. S. Transgenic amplification of glucocorticoid action in adipose tissue causes high blood pressure in mice. *J. Clin. Invest.* **2003**, *112*, 83–90.
- (15) Paterson, J. M.; Morton, N. M.; Fievet, C.; Kenyon, C. J.; Holmes, M. C.; Staels, B.; Seckl, J. R.; Mullins, J. J. Metabolic syndrome without obesity: Hepatic overexpression of 11 $\beta$ -hydroxysteroid dehydrogenase type 1 in transgenic mice. *Proc. Natl. Acad. Sci. U.S.A.* **2004**, *101*, 7088–7093.
- (16) Kershaw, E. E.; Morton, N. M.; Dhillon, H.; Ramage, L.; Seckl, J. R.; Flier, J. S. Adipocyte-specific glucocorticoid inactivation protects against diet-induced obesity. *Diabetes* **2005**, *54*, 1023–1031.
- (17) Morton, N. M.; Ramage, L.; Seckl, J. R. Down-regulation of adipose 11 $\beta$ -hydroxysteroid dehydrogenase type 1 by high-fat feeding in mice: A potential adaptive mechanism counteracting metabolic disease. *Endocrinology* **2004**, *145*, 2707–2712.
- (18) (a) Rask, E.; Olsson, T.; Soderberg, S.; Andrew, R.; Livingstone, D. E. W.; Johnson, O.; Walker, B. R. Tissue-specific dysregulation of cortisol metabolism in human obesity. *J. Clin. Endocrinol. Metab.* **2001**, *86*, 1418–1421. (b) Paulmyer-Lacroix, O.; Boullu, S.; Oliver, C.; Alessi, M.-C.; Grino, M. Expression of the mRNA coding for 11 $\beta$ -hydroxysteroid dehydrogenase type 1 in adipose tissue from obese patients: An in situ hybridization study. *J. Clin. Endocrinol. Metab.* **2002**, *87*, 2701–2705. (c) Rask, E.; Walker, B. R.; Soderberg, S.; Livingstone, D. E. W.; Eliasson, M.; Johnson, O.; Andrew, R.; Olsson, T. Tissue-specific changes in peripheral cortisol metabolism in obese women: Increased adipose 11 $\beta$ -hydroxysteroid dehydrogenase type 1 activity. *J. Clin. Endocrinol. Metab.* **2002**, *87*, 3330–3336. (d) Lindsay, R. S.; Wake, D. J.; Nair, S.; Bunt, J.; Livingstone, D. E. W.; Permana, P. A.; Tataranni, P. A.; Walker, B. R. Subcutaneous adipose 11 $\beta$ -hydroxysteroid dehydrogenase type 1 activity and messenger ribonucleic acid levels are associated with adiposity and insulinemia in Pima Indians and Caucasians. *J. Clin. Endocrinol. Metab.* **2003**, *88*, 2738–2744. (e) Wake, D. J.; Rask, E.; Livingstone, D. E. W.; Soederberg, S.; Olsson, T.; Walker, B. R. Local and systemic impact of transcriptional up-regulation of 11 $\beta$ -hydroxysteroid dehydrogenase type 1 in adipose tissue in human obesity. *J. Clin. Endocrinol. Metab.* **2003**, *88*, 3983–3988. (f) Engeli, S.; Bohnke, J.; Feldpausch, M.; Gorzelniak, K.; Heintze, U.; Janke, J.; Luft, F. C.; Sharma, A. M. Regulation of 11 $\beta$ -HSD genes in human adipose tissue: influence of central obesity and weight loss. *Obes. Res.* **2004**, *12*, 9–17. (g) Kannisto, K.; Pietilaenen, K. H.; Ehrenborg, E.; Rissanen, A.; Kaprio, J.; Hamsten, A.; Yki-Jaervinen, H. Overexpression of 11 $\beta$ -hydroxysteroid dehydrogenase-I in adipose tissue is associated with acquired obesity and features of insulin resistance: Studies in young adult monozygotic twins. *J. Clin. Endocrinol. Metab.* **2004**, *89*, 4414–4421. (h) Sandeep, T. C.; Andrew, R.; Homer, N. Z. M.; Andrews, R. C.; Smith, K.; Walker, B. R. Increased in vivo regeneration of cortisol in adipose tissue in human obesity and effects of the 11 $\beta$ -hydroxysteroid dehydrogenase type 1 inhibitor carbenoxolone. *Diabetes* **2005**, *54*, 872–879.
- (19) Tomlinson, J. W.; Sinha, B.; Bujalska, I.; Hewison, M.; Stewart, P. M. Expression of 11 $\beta$ -hydroxysteroid dehydrogenase type 1 in adipose tissue is not increased in human obesity. *J. Clin. Endocrinol. Metab.* **2002**, *87*, 5630–5635.
- (20) Stewart, P. M.; Boulton, A.; Kumar, S.; Clark, P. M. S.; Shackleton, C. H. L. Cortisol metabolism in human obesity: Impaired cortisone  $\rightarrow$  cortisol conversion in subjects with central adiposity. *J. Clin. Endocrinol. Metab.* **1999**, *84*, 1022–1027.
- (21) Purnell, J. Q.; Brandon, D. D.; Isabelle, L. M.; Loriaux, D. L.; Samuels, M. H. Association of 24-hour cortisol production rates, cortisol-binding globulin, and plasma-free cortisol levels with body composition, leptin levels, and aging in adult men and women. *J. Clin. Endocrinol. Metab.* **2004**, *89*, 281–287.
- (22) (a) Andrew, R.; Smith, K.; Jones, G. C.; Walker, B. R. Distinguishing the activities of 11 $\beta$ -hydroxysteroid dehydrogenases in vivo using isotopically labeled cortisol. *J. Clin. Endocrinol. Metab.* **2002**, *87*, 277–285. (b) Basu, R.; Singh, R. J.; Basu, A.; Chittilapilly, E. G.; Johnson, C. M.; Toffolo, G.; Cobelli, C.; Rizza, R. A. Splanchnic cortisol production occurs in humans: Evidence for conversion of cortisone to cortisol via the 11 $\beta$ -hydroxysteroid dehydrogenase (11 $\beta$ -HSD) type 1 pathway. *Diabetes* **2004**, *53*, 2051–2059. (c) Andrew, R.; Westerbacka, J.; Wahren, J.; Yki-Jaervinen, H.; Walker, B. R. The contribution of visceral adipose tissue to splanchnic cortisol production in healthy humans. *Diabetes* **2005**, *54*, 1364–1370. (d) Basu, R.; Singh, R. J.; Basu, A.; Chittilapilly, E. G.; Johnson, C. M.; Toffolo, G.; Cobelli, C.; Rizza, R. A. Obesity and type 2 diabetes do not alter splanchnic cortisol production in humans. *J. Clin. Endocrinol. Metab.* **2005**, *90*, 3919–3926.
- (23) (a) Chrousos, G. P. Is 11 $\beta$ -hydroxysteroid dehydrogenase type 1 a good therapeutic target for blockade of glucocorticoid actions? *Proc. Natl. Acad. Sci. U.S.A.* **2004**, *101*, 6329–6330. (b) Davies, E.; MacKenzie, S. M. Extra-adrenal production of corticosteroids. *Clin. Exp. Pharmacol. Physiol.* **2003**, *30*, 437–445. (c) Giordano, R.; Pellegrino, M.; Picu, A.; Bonelli, L.; Balbo, M.; Berardelli, R.; Lanfranco, F.; Ghigo, E.; Arvat, E. Neuroregulation of the hypothalamus-pituitary-adrenal (HPA) axis in humans: Effects of GABA-, mineralocorticoid-, and GH-secretagogue-receptor modulation. *The-ScientificWorld* **2006**, *6*, 1–11. (d) Swaab, D. F.; Bao, A.-M.; Lucassen, P. J. The stress system in the human brain in depression and neurodegeneration. *Ageing Res. Rev.* **2005**, *4*, 141–194. (e) Buckley, T. M.; Schatzberg, A. F. Review: On the interactions of the hypothalamic-pituitary-adrenal (HPA) axis and sleep: Normal HPA axis activity and circadian rhythm, exemplary sleep disorders. *J. Clin. Endocrinol. Metab.* **2005**, *90*, 3106–3114.
- (24) Human and rodent species differences in androgen metabolism and function are known. (a) Karsch, F. J.; Dierschke, D. J.; Knobil, E. Sexual differentiation of pituitary function: Apparent difference between primates and rodents. *Science* **1973**, *179*, 484–486. (b) Grino, M. Adrenal cortex, development. *Encycl. Endocr. Dis.* **2004**, *1*, 53–60. (c) Smith, C. J.; Norman, R. L. Circadian periodicity in circulating cortisol is absent after orchidectomy in rhesus macaques. *Endocrinology* **1987**, *121*, 2186–2191.
- (25) Harris, H. J.; Kotelevtsev, Y.; Mullins, J. J.; Seckl, J. R.; Holmes, M. C. Intracellular regeneration of glucocorticoids by 11 $\beta$ -hydroxysteroid dehydrogenase (11 $\beta$ -HSD)-1 plays a key role in regulation of the hypothalamic-pituitary-adrenal axis: Analysis of 11 $\beta$ -HSD-1-deficient mice. *Endocrinology* **2001**, *142*, 114–120.
- (26) Wang, M. Inhibitors of 11 $\beta$ -hydroxysteroid dehydrogenase type 1 for the treatment of metabolic syndrome. *Curr. Opin. Invest. Drugs* **2006**, *7*, 319–323 and reference contained therein to Paterson, J. Studies of 11 $\beta$ -Hydroxysteroid dehydrogenase type 1 in transgenic mouse models. Glucocorticoid Activation as a Pharmacological Target in Metabolic Disease Conference, Stockholm, Sweden, 2005.
- (27) (a) Livingstone, D. E. W.; Walker, B. R. Is 11 $\beta$ -hydroxysteroid dehydrogenase type 1 a therapeutic target? Effects of carbenoxolone in lean and obese Zucker rats. *J. Pharmacol. Exp. Ther.* **2003**, *305*, 167–172. (b) Andrews, R. C.; Rooyackers, O.; Walker, B. R. Effects of the 11 $\beta$ -hydroxysteroid dehydrogenase inhibitor carbenoxolone on insulin sensitivity in men with type 2 diabetes. *J. Clin. Endocrinol. Metab.* **2003**, *88*, 285–291. (c) Sandeep, T. C.; Yau, J. L. W.; MacLulich, A. M. J.; Noble, J.; Deary, I. J.; Walker, B. R.; Seckl, J. R. 11 $\beta$ -Hydroxysteroid dehydrogenase inhibition improves cognitive function in healthy elderly men and type 2 diabetics. *Proc. Natl. Acad. Sci. U.S.A.* **2004**, *101*, 6734–6739.
- (28) (a) Barf, T.; Vallgarda, J.; Emond, R.; Haggstrom, C.; Kurz, G.; Nygren, A.; Larwood, V.; Mosialou, E.; Axelsson, K.; Olsson, R.; Engblom, L.; Edling, N.; Ronquist-Nii, Y.; Ohman, B.; Alberts, P.; Abrahmsen, L. Arylsulfonamidothiazoles as a new class of potential antidiabetic drugs. Discovery of potent and selective inhibitors of the 11 $\beta$ -hydroxysteroid dehydrogenase type 1. *J. Med. Chem.* **2002**, *45*, 3813–3815. (b) Alberts, P.; Engblom, L.; Edling, N.; Forsgren, M.; Klingstrom, G.; Larsson, C.; Ronquist-Nii, Y.; Ohman, B.; Abrahmsen, L. Selective inhibition of 11 $\beta$ -hydroxysteroid dehydrogenase type 1 decreases blood glucose concentrations in hyperglycaemic mice. *Diabetologia* **2002**, *45*, 1528–1532. (c) Alberts, P.; Nilsson, C.; Selen, G.; Engblom, L. O. M.; Edling, N. H. M.; Norling, S.; Klingstrom, G.; Larsson, C.; Forsgren, M.; Ashkzari, M.; Nilsson, C. E.; Fiedler, M.; Bergqvist, E.; Ohman, B.; Bjorkstrand, E.; Abrahmsen, L. B. Selective inhibition of 11 $\beta$ -hydroxysteroid dehydrogenase type 1 improves hepatic insulin sensitivity in hyperglycaemic mice strains. *Endocrinology* **2003**, *144*, 4755–4762.
- (29) (a) Olson, S.; Aster, S. D.; Brown, K.; Carbin, L.; Graham, D. W.; Hermanowski-Vosatka, A. H.; LiGrand, C. B.; Mundt, S. S.; Robbins, M. A.; Schaeffer, J. M.; Slossberg, L. H.; Szymonifka, M. J.; Thieringer, R.; Wright, S. D.; Balkovec, J. M. Adamantyl triazoles as selective inhibitors of 11 $\beta$ -hydroxysteroid dehydrogenase type 1. *Bioorg. Med. Chem. Lett.* **2005**, *15*, 4359–4362. (b) Hermanowski-Vosatka, A. H.; Balkovec, J. M.; Cheng, K.; Chen, H. Y.; Hernandez, M.; Koo, G. C.; Le Grand, C. B.; Li, Z.; Metzger, J. M.; Mundt, S. S.; Noonan, H.; Nunes, C. N.; Olson, S. H.; Pikounis, B.; Ren, N.;

- Robertson, N.; Schaeffer, J. M.; Shah, K.; Springer, M. S.; Strack, A. M.; Strowski, M.; Wu, K.; Wu, T.; Xiao, J.; Zhang, B. B.; Wright, S. D.; Thieringer, R.  $11\beta$ -HSD1 inhibition ameliorates metabolic syndrome and prevents progression of atherosclerosis in mice. *J. Exp. Med.* **2005**, *202*, 517–527.
- (30) Yau, J. L. W.; Noble, J.; Kenyon, C. J.; Hibberd, C.; Kotelevtsev, Y.; Mullins, J. J.; Seckl, J. R. Lack of tissue glucocorticoid reactivation in  $11\beta$ -hydroxysteroid dehydrogenase type 1 knockout mice ameliorates age-related learning impairments. *Proc. Natl. Acad. Sci. U.S.A.* **2001**, *98*, 4716–4721.
- (31) Rauz, S.; Cheung, C. M. G.; Wood, P. J.; Coca-Prados, M.; Walker, E. A.; Murray, P. I.; Stewart, P. M. Inhibition of  $11\beta$ -hydroxysteroid dehydrogenase type 1 lowers intraocular pressure in patients with ocular hypertension. *QJM: Monthly Journal of the Association of Physicians* **2003**, *96*, 481–490.
- (32) Cai, T.-Q.; Wong, B.; Mundt, S. S.; Thieringer, R.; Wright, S. D.; Hermanowski-Vosatka, A. Induction of  $11\beta$ -hydroxysteroid dehydrogenase type 1 but not -2 in human aortic smooth muscle cells by inflammatory stimuli. *J. Steroid Biochem. Mol. Biol.* **2001**, *77*, 117–122.
- (33) Cooper, M. S.; Rabbitt, E. H.; Goddard, P. E.; Bartlett, W. A.; Hewison, M.; Stewart, P. M. Osteoblastic  $11\beta$ -hydroxysteroid dehydrogenase type 1 activity increases with age and glucocorticoid exposure. *J. Bone Miner. Res.* **2002**, *17*, 979–986.
- (34) Nilsson, C.; Dreifeldt, C. Method for promoting impaired wound healing. PCT Int. Appl. WO2004112785, 2004.
- (35) Tomlinson, J. W.  $11\beta$ -hydroxysteroid dehydrogenase type 1 in human disease: A novel therapeutic target. *Minerva Endocrinol.* **2005**, *30*, 37–46.
- (36) Espino, C. G.; Du Bois, J. A Rh-catalyzed C–H insertion reaction for the oxidative conversion of carbamates to oxazolidinones. *Angew. Chem., Int. Ed.* **2001**, *40*, 598–600.
- (37) Kocovsky, P. Carbamates: A method of synthesis and some synthetic applications. *Tetrahedron Lett.* **1986**, *27*, 5521–5524.
- (38) Jones, C. D.; Kaselj, M.; Salvatore, R. N.; le Noble, W. J. Effects of substituent modification on face selection in reduction. *J. Org. Chem.* **1998**, *63*, 2758–2760.
- (39) Fischer, W.; Grob, C. A.; Katayama, H. The synthesis of 1,3-disubstituted adamantanes. *Helv. Chim. Acta* **1976**, *59*, 1953–1962.
- (40) Jasys, V. J.; Lombardo, F.; Appleton, T. A.; Bordner, J.; Ziliox, M.; Volkmann, R. A. Preparation of fluoroadamantane acids and amines: Impact of bridgehead fluorine substitution on the solution- and solid-state properties of functionalized adamantanes. *J. Am. Chem. Soc.* **2000**, *122*, 466–473.
- (41) Bhatia, P. A.; Daanen, J. F.; Hakeem, A. A.; Kolasa, T.; Matulenko, M. A.; Mortell, K. H.; Patel, M. V.; Stewart, A. O.; Wang, X.; Xia, Z.; Zhang, H. Q. Preparation of piperazinyl, piperidinyl and related acetamides and benzamides as dopamine D4 receptor agonists useful in treating sexual dysfunction. U.S. Pat. Appl. Publ. US2003229094, 2003.
- (42) (a) Tsuzuki, N.; Hama, T.; Kawada, M.; Hasui, A.; Konishi, R.; Shiwa, S.; Ochi, Y.; Futaki, S.; Kitagawa, K. Adamantane as a brain-directed drug carrier for poorly absorbed drug. 2. AZT derivatives conjugated with the 1-adamantane moiety. *J. Pharm. Sci.* **1994**, *83*, 481–484. (b) Tsuzuki, N.; Hama, T.; Hibi, T.; Konishi, R.; Futaki, S.; Kitagawa, K. Adamantane as a brain-directed drug carrier for poorly absorbed drug: Antinociceptive effects of [D-Ala2]Leu-enkephalin derivatives conjugated with the 1-adamantane moiety. *Biochem. Pharmacol.* **1991**, *41*, R5–R8. (c) Wishnok, J. S. Medicinal properties of adamantane derivatives. *J. Chem. Educ.* **1973**, *50*, 780–781.
- (43) (a) White, R. E.; McCarthy, M.-B.; Egeberg, K. D. Sligar, S. G. Regioselectivity in the cytochromes P-450: Control by protein constraints and by chemical reactivities. *Arch. Biochem. Biophys.* **1984**, *228*, 493–502. (b) Raag, R.; Poulos, T. L. Crystal structures of cytochrome P-450<sub>CAM</sub> complexed with camphane, thiocamphor, and adamantane: Factors controlling P-450 substrate hydroxylation. *Biochemistry* **1991**, *30*, 2674–2684.
- (44) Receptor binding assays performed by CEREP ([www.cerep.com](http://www.cerep.com)).
- (45) Ziegler, F. E.; Fowler, K. W. Substitution reactions of specifically ortho-metalated piperonal cyclohexylimine. *J. Org. Chem.* **1976**, *41*, 1564–1566.
- (46) Obach, R. S. Prediction of human clearance of twenty-nine drugs from hepatic microsomal intrinsic clearance data: an examination of in vitro half-life approach and nonspecific binding to microsomes. *Drug Metab. Dispos.* **1999**, *27*, 1350–1359.
- (47) Gao, L.; Chiou, W.; Cheng, X.; Camp, H.; Burns, D. Quantification Of corticosteroids from ex vivo activity assay. Proceedings of the 54th ASMS Conference on Mass Spectrometry, Seattle, WA, U.S.A., May 29–June 1, 2006.

JM0609364